Mechanical properties of Pd, Pt and its alloy nanowires studied by molecular dynamics simulations

A thesis submitted in partial fulfilment of the
Requirements for the degree of

Master of technology
in
Metallurgical and Materials Engineering

By

JAY KRISHAN DORA (212MM1448)

Department of Metallurgical and Materials Engineering
National Institute of Technology
Rourkela
2014

Mechanical properties of Pd, Pt and its alloy nanowires studied by molecular dynamics simulations

A thesis submitted in partial fulfilment of the
Requirements for the degree of

Master of technology
in
Metallurgical and Materials Engineering

By

JAY KRISHAN DORA (212MM1448)

Under the guidance of

Prof. NATRAJ YEDLA

Department of Metallurgical and Materials Engineering
National Institute of Technology
Rourkela
2014

DEPARTMENT OF METALLURGICAL & MATERIALS ENGINEERING
NATIONAL INSTITUTE OF TECHNOLOGY

ROURKELA-769008, INDIA

CERTIFICATE

This is to certify that the project entitled "**Mechanical properties of Pd, Pt and its alloy nanowires studied by molecular dynamics simulations** submitted by **Mr. JAY KRISHAN DORA (212MM1448)** in partial fulfilments for the needs for the award of **Master of Technology** Degree in **Metallurgical & Materials Engineering** at **National Institute of Technology, Rourkela** is an authentic work executed by him under my direction and guidance. To the best of my awareness, the substance embodied in the report has not been submitted to any other University / Institute for the award of any Degree.

DATE: 27.05.2014

Prof. N. YEDLA
Department of Metallurgical & Materials Engineering
National Institute of Technology
Rourkela-769008

ACKNOWLEDGEMENT

I would like to show gratitude to **NIT Rourkela** for giving me the prospect to utilize its assets and work in such an exigent environment. First and foremost, I take this chance to articulate my profound regards and honest gratefulness to my guide **Prof. N. Yedla** for his proficient supervision and invariable support throughout my project work. This project would not have been achievable without his aid and the priceless time that he has given me amidst his tiring schedule.

I would also like to express my paramount gratitude to **Prof. B.C Ray, HOD, Metallurgical & Materials engineering** for permitting me to use the departmental amenities.

I would also like to extend my jovial gratefulness to my associates and superior students of this branch who always encouraged and supported me in undertaking my work. Last but not the least; I would like to thank all the employees of Department of Metallurgical &Materials Engineering who were incredibly cooperative with me.

Place: NIT-Rourkela ***Jay Krishan Dora***

Date: 27.05.2014

ABSTRACT

The research work carried out in this thesis with the help of molecular dynamics (MD) simulation techniques to study the mechanical properties of Pd, Pt and Pd_{50}-Pt_{50} alloy nanowire. Classical molecular dynamics simulation deformation studies of Pd, Pt and Pd_{50}-Pt_{50}were acted upon using LAMMPS (Large scale atomic/molecular massively parallel simulator). The ductile nature of Pd, Pt and its alloy nanowire is observed through a series of VMD (visual molecular dynamics) snapshots taken at different strains. Mechanical properties were evaluated by subjecting the nanowires to uniaxial tensile deformation at varying strain rates and temperature. It was found that nanowires were sensitive to strain rate and temperature conditions. There are five strain rates (1%, 3%, 5%, 8%,and 10% ps^{-1}) at which MD simulations have been done. Also tensile deformation has been done at four different temperatures (100K, 300K, 500K, and 700K). Strain rate sensitivity of the mentioned nanowire is also evaluated. It is found that strain rate sensitivity fluctuates with respect to temperature.

Keywords: Molecular dynamics, LAMMPS, Mechanical properties, Strain rate sensitivity.

CONTENTS **Page no.**

CHAPTER -1

INTRODUCTION

1. Introduction

1.1.Background

Nanotechnology is the knowing and manipulating the matter dimension between 1 and 100 nanometre. Unique properties of the materials are found in the nano-scale. Nanowires are one of the exciting nanomaterials, having the diameter in the order of nanometre scale i.e. 10^{-9} meters. Nanowires are basically referred as a 1D structure which exhibits one or more than 1000 as length to width ratio, Nanowire can also be defined as the structure having diameter or thickness limited to some nanometre or less, these scales are responsible for the quantum mechanical effect, so nanowire is also termed as quantum wires. Presently, Nanowire is preferred over bulk materials because of their unique properties. The primary cause responsible for its extraordinary behaviour is due to the presence of electrons in the quantum level, these electrons occupy the energy level different from the bands found in bulk materials or continuum level. Nanowire has very high surface area to the volume ratio in the nanometre scale, this characteristic helps nanowire exhibiting superior properties. Physical properties of a material is mainly effected by surface energy and surface stresses, which correspondingly depends upon the configuration and orientation of the structure. In nanometre scale, role of surfaces plays crucial role in influencing the mechanical properties and the characteristic of plastic deformation as compared to its bulk counterparts. There are different types of nanowire, which includes, metallic nanowire like, (Palladium, Nickel, Platinum, gold etc), Semiconducting nanowire, Insulating nanowire like, (silicon oxide, titanium oxide etc) and molecular nanowire, this includes inorganic and organic molecular units. Here, our focus is on metallic nanowire. Metallic nanowire has prevalent relevance because of its superior mechanical, electrical and magnetic properties [1]. Metallic nanowire is also applicable in the field of nano-electronics, optoelectronics [2] and nano-mechanical devices [3]. Metallic nanowires are also used in composite materials in the form of reinforcement for high strength and light weight [4], catalysis, nano-pipette probes, superconductors [5] and they have also been applicable as the tips for scanning tunnelling and atomic force microscopes [6]. The widespread and impressive applications of metallic nanowire compelled the inventors to study its properties.

1.2 Idea for the present study

The most common way to find the mechanical properties of materials is to execute physical experiments. Mechanical properties like Young's modulus, yield stress, and yield strain for any metallic systems are generally considered. These are the properties that are independent of size or shape. But the mechanical properties of the metallic systems depends on the size and shape in the nanometre scale. Several interesting engineering opportunities arise due to size and shape dependence. If the concepts of the mechanisms causing the variations are developed, then the desirable materials may be developed for the required physical properties based on application. There is a limit to extract the information's due to extremely small dimension of metallic nanowires, the experiments conducted faced numerous drawbacks like, expensive setups to maintain the high precision equipments/facilities; complications and uncertainty in nano-scale measurements and the important one is, the experimentally studying the deformation phenomenon is still out of reach; which is the greatest barrier in finding the properties of metallic nanowires. For these reasons, numerical simulation study is highly essential. As an alternative to physical experiments, presently, Molecular dynamics simulation study is a primary means for investigating the mechanical properties of nanowires and the related mechanisms. Basically, molecular dynamics simulation study has the ability to simulate a system and finding the behaviour in the nanoscale deformation process. These advantages of molecular dynamics simulation technique made it very demanding in the various fields like; physics, chemistry, biology, materials science etc. These simulation experiments can be executed to allow the experts to view the movement of individual atoms throughout the structure. At very small time steps, the computer programs can calculate a large number of physical quantities. These atomistic simulations have focused on characterizing the influence of mechanical properties of metallic nanowires. Some previous works illustrates the work of molecular dynamics simulation technique to find the mechanical properties of cylindrical bimetallic Pd-Pt nanowires for two dissimilar compositions i.e. Pt content of 25% and 50% and an estimated1.4 nm as diameter of the same. Uniaxial tensile strain with changing strain rates of 0.05% $ps^{-1}$and 5.0% ps^{-1} are provided to the mentioned nanowire, at the temperature ranges between 50 K and 300 K and study the effects of strain rates and thermal conditions on the and mechanical properties of the nanowire [6]. Similarly, the effects of strain rates (0.04%, 0.4% and 4%) and thermal conditions (50 K and 300 K) of platinum nanowire on the mechanical properties of the same were also studied [7]. It is seen that molecular dynamics (MD) simulation technique is playing a vital role in the study of

materials properties. Valuable works has been done to investigate the values of the various mechanical properties for metallic nanowires. But, there are some key differences that set this work apart from other works. Previously, we see that there is a comparison between the metallic nanowires in terms of compositions and limited strain rates and temperature range. However, our work is based on the comparison between Pt_{50}-Pt_{50}alloys and individual Pd and Pt at various temperature range and strain rate values. So, the molecular dynamics simulation studies have been carried out to overcome the gaps.

1.3 Research objective

(a) To study the effect of temperature on the mechanical properties of Pd, Pt, and Pd-Pt alloy nanowires.
(b) To study the effect of strain rate on the mechanical properties of Pd, Pt, and Pd-Pt alloy nanowires.
(c) To study the variations in strain rate sensitivity with respect to temperature of Pd, Pt, and Pd-Pt alloy nanowires.

Chapter-2

Literature Survey

2 Literature Survey

2.1 History

In the year 1959, the term nanotechnology was proposed by Richard Feyman. He described it as a process which is capable of manipulating the individual atoms and molecules. It uses a set of precise tools to develop another smaller set and so on needed smaller scale too. (Feyman, 1960). In the year 1974, this term "Nanotechnology" called as a precise and accurate tolerance needed for machining and finishing materials. In the year 1986, the term "Nanotechnology" came into existence due to contribution by Drexler (Drexler and Minsky, 1990). Nanotechnology was referred widely and enormously since then as a most crucial technology. Some illustrations like, in the field of electronics integrated circuits are based on some features in the 30nm range and even smaller, which is many times smaller than the biological cells. These devices and materials have promising applications in the area of chemistry, energy, health, electronics, and heavy industries and so on [8].

Nanowires are especially attractive for the promising role in nano-science studies as well as for nanotechnology. However, nanowires exclusive density, small diameters makes it very significant in the form of the properties like optical, magnetic, chemical etc as compared to its bulk counterparts.

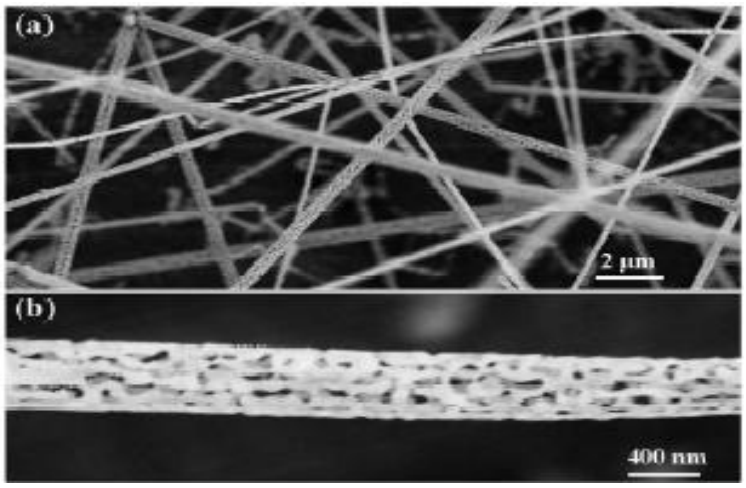

Figure 2.1: Schematic view of nanowires a) Mesoporous ZnO Nanowires. b) Single crystal ZnO nanowires [9].

2.2 Fabrication of nanowires [9]

Basically, these fabrication techniques are divided into following four groups:

1) Electro-spinning.
2) Lithography.
3) Spontaneous growth includes :

Evaporation condensation, Dissolution condensation, Vapor-Liquid-Solid growth (VLS), Stress induced re-crystallization.

4) Template-based synthesis includes:

Electrochemical deposition, Electrophoretic deposition, Colloid dispersion, Conversion with chemical reaction.

2.2.1 Electro-spinning

The electrical forces at the surface are responsible for electro-spinning of a polymer solution or melt to conquer the surface tension and ejection of electrically charged jet is carried out. The solidification of jet tends to remains of electrically charged fibre. Acceleration of this fibre is carried out by electrical forces and then serene in sheets in the required geometrical appearance.

2.2.2 Lithography

Various lithography techniques have been developed such as electron beam lithography, ion beam lithography, X-ray lithography in the fabrication of nanowires. The diameter of nanowires i.e.10 nm or less and 100 as an aspect ratio can be set.

2.2.3 Spontaneous Growth

Gibbs free energy or chemical potential drop is a defined by spontaneous growth process. The formation of nanowires is a direction dependant growth (i.e. the crystal along a definite course is more rapid than erstwhile directions). The Gibbs free energy decline is generally occurred by phase change or chemical response or by stress release. Uniform sized nanowires i.e. having the identical diameter along the longitudinal path of a nanowire can be found that growth proceeds unidirectional, but there is no growth along the other direction.

2.2.3.1 Evaporation condensation

This process is also known as Vapor-Solid (VS) technique. Nanowires grown by this method are basically solo crystals amid very less imperfections. The development of nanowires

happens due to the anisotropic growth. The diverse aspects in a crystal have dissimilar growth rates. There is no control on the direction of growth of nanowire in this method.

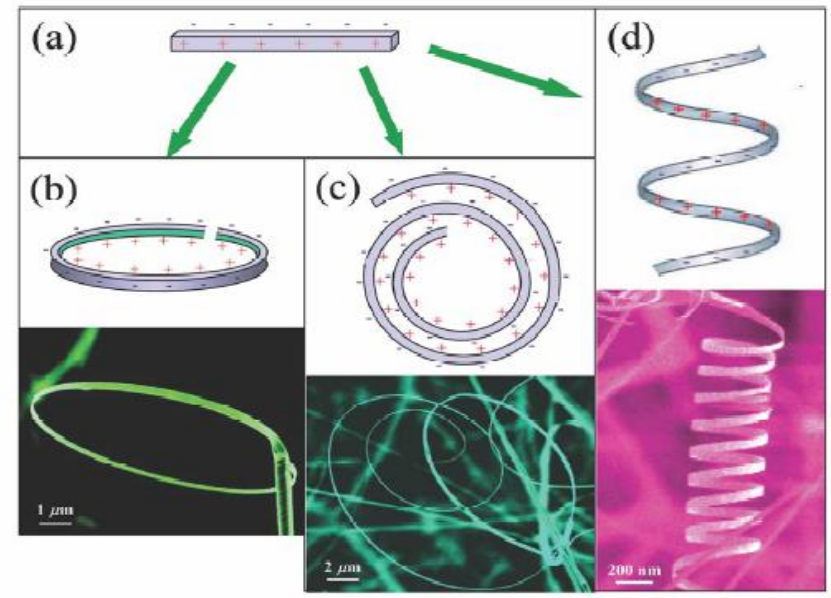

Figure 2.2: (a) Replica of a polar nanobelt. (b) nanorings, (c) nanospirals, and(d) nanohelixes of Zinc Oxide and their development methods [9].

2.2.3.2 Dissolution condensation

In the solution the growth species is dissolved and deposited on the exterior, consequently the development of nanowires occurs. A mean length of less than 500 nm and a mean diameter of about 60 nm nanowires can be fabricated in this method.

2.2.3.3 Vapour-Liquid-Solid growth

In VLS growth, a catalyst is termed as a second phase material. It progress and limit the crystal growth on a particular course and within a limited region. A liquid globule is formed by a catalyst and also by alloy treatment in addition with enlargement matter during the growth process. Improved developed species in the catalyst bead later precipitates at the augmented face ensuing the one-directional intensification (figure 2.3). In this process, the species grown is first evaporated then dissolves and diffuses into a liquid drip. The liquid exterior has largely dwelling coefficient, so a suitable site for deposition is confirmed. The precipitate at the interface (i.e. between the substrate and liquid) and diffusion of liquid droplet is occurred in saturated growth species. Repeated growth and precipitation separates the liquid droplet and substrate, which infers in the creation of nanowires. The nanowires can

have the nominal diameters of about 5 nm and a span altering from little tens to several hundred micrometers.

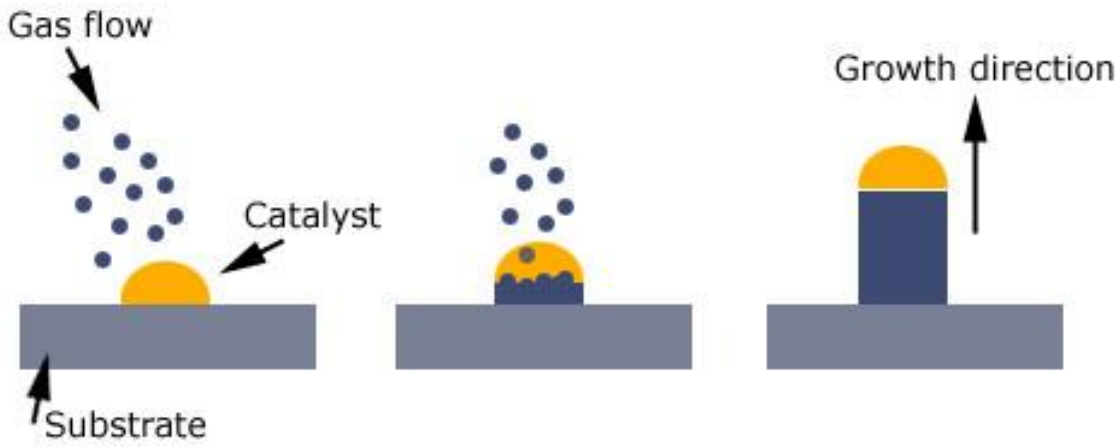

Figure 2.3: Representation of VLS growth [9]

2.2.4 Template Based Synthesis

This method is applicable to fabricate the nanowires of polymers, metals, semiconductors, and oxides. The fabrications of porous membranes are done with different methods. The target densities are attained as high as 1011 pores/cm^2 by the arrangements of pores in regular hexagonal arrays. The range of pore dimension from 10 nm to 100 mm can be accomplished.

2.2.4.1Electrochemical Deposition

2.2.4.1.1 Negative Template

Solid material as templates is used by a prefabricated cylindrical nanopore. To form nanowires, there are various ways to fill the nano-pores, but the electrochemical method is the most suitable method. Fabrication of suitable templates is clearly a critical first step. On one side of a membrane, metal film is required for electro deposition to act as a working electrode. Nanowires are obtained when host of solid material is dissolved. The diameter of the nanowires is calculated by the geometrical constraint of the pores.

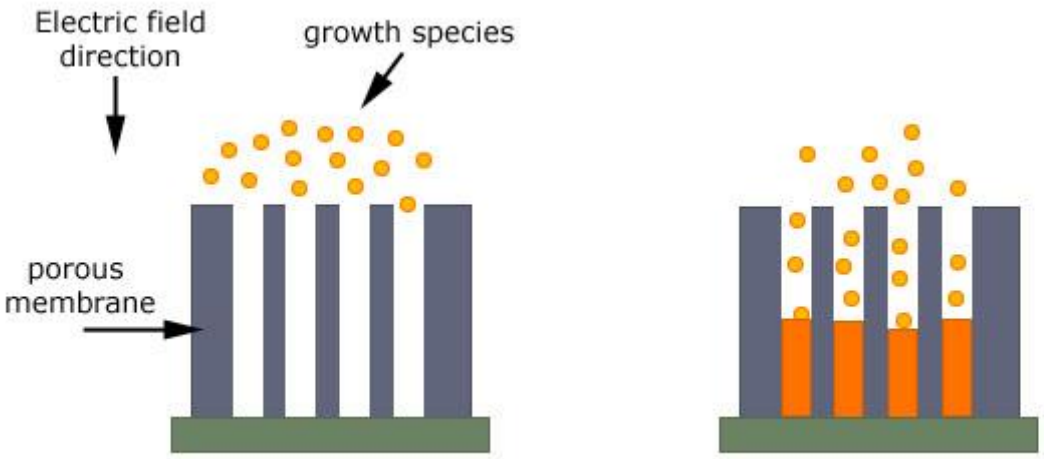

Figure 2.4: Representation of template base synthesis [9].

2.2.4.1.2 Positive Template Method

In this method DNA and carbon nano-tubes are used as templates. On the external facade of the templates nanowires are formed. Nanowire diameter is not constrained by the template dimension; it is restricted by manipulating the quantity of materials dumped on the templates. After removal of templates, wire-like and tube-like configuration can be fashioned. Nanowires are figured on the external face of the templates. Template in the form of DNA is the best choice to formulate nanowires as its diameter is about 2 nm and its span and order can be properly guarded. It is done by fixing a DNA filament between two electrical connections; the DNA is subsequently treated with solution having some ions. Binding of ions to DNA then forms some nano-particles sequencing along the DNA chain. Later, these nano-particles are then extended into a nanowire by means of a yardstick photographic enhancement method.

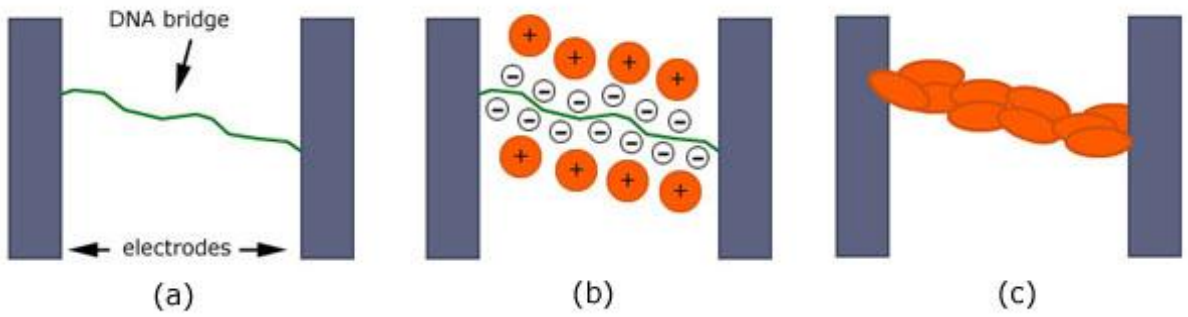

Figure 2.5: DNA base template (a) DNA overpass linking two electrodes, (b) Ion encumbered DNA link, (c) Wholly developed wire on DNA [9].

2.2.4.2 Electrophoretic Deposition

In this method, electrically conductive deposit is not required; hence this method is particularly useful for fabricating oxide nanowires such as SiO_2, TiO_2, Bi_2O_3, etc. in colloidal dispersions nano-size particles are characteristically controlled by electrostatic means. Over the facade of nano-particles an electrical charge is developed through some chemical techniques. External electric field is applied to a system of charged nano size particle; due to the electric field the particles are put in movement. This type of action is called as electrophoresis; the remaining technique is as similar as electrochemical deposition.

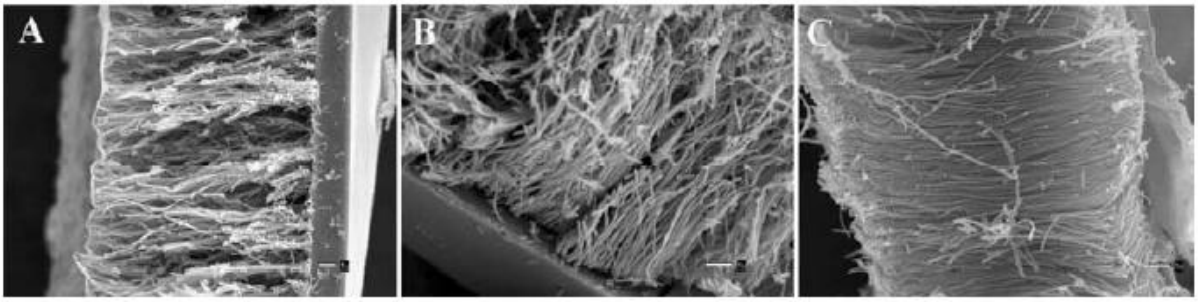

Figure 2.6: Diverse sizes of TiO_2 nano-rods matured in a casing by sol electro-phoretic deposition. Diameters: (A) 180 nm, (B) 90 nm, (C) 45 nm [9].

2.2.2.3 Surface Step-Edge Templates

Along a crystal surface atomic-scale steps can be used as the templates for the growth of nanowires. The deposition of various materials on the surface starts preferentially at defect sites, such as exterior step-edges hence this method is also called as step edge decoration. Fabrication of nanowires is done by electro-deposition, step edges of highly oriented graphite as template is used. Different method such as physical vapour deposition (PVD) method is also used. The major problem faced by the nanowires is that, it is hardly removed from the surface of deposition. However, there are various techniques for separating the nanowires form the edge of the substrate crystal.

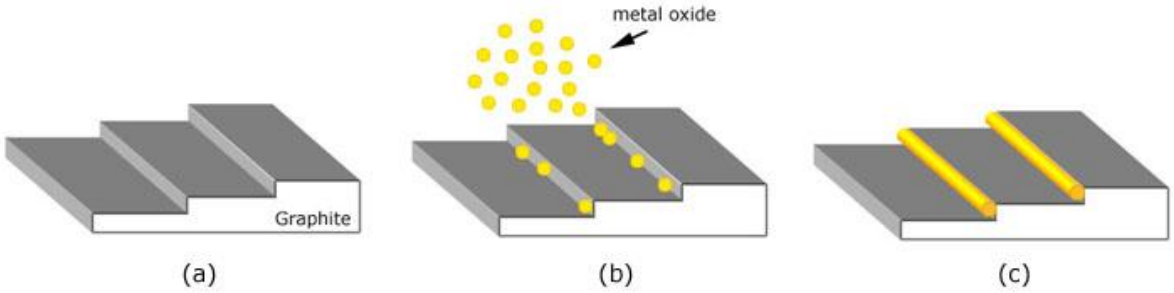

Figure 2.7 Surface step-edge template (a) step-edge graphite, (b) Electro-deposition of metal oxide, (c) Creation of nanowire at the edges [9].

2.3 In-situ experiment conducted

Tensile testing is a versatile experimental technique to evaluate the mechanical properties like plasticity, elasticity and failure. The concept behind the in-situ test is, initially, the specimen is fixed/ clamped on a nano-manipulator tip and the force is applied on the free end. During the loading, the AFM cantilever is used to measure the strain or elongation in the other side. This can be carried out in a Transmission electron microscopy (TEM) and Scanning electron microscopy (SEM) [10]. The silicon nanowires having diameter in the range of 15 and 60 nm has been investigated by various tensile experiments [11] to calculate modulus and fracture strength. The nanowires ranging from 1.5 to 4.3μm have also been investigated for the derivation of young's modulus. In the zinc oxide nanowires the elastic failure properties was studied by [11] under tension and compression. reported that the Copper nanowires were fabricated using high temperature molecular beam epitaxy method, which shows strength close to theoretical tension tests conducted reported by [12]. Current studies regarding gold nanowires [13] have also been reported.

2.4 Gaps in the experiment

Structure-property association of nanowires was evaluated by in situ experiments and has emerged as a commanding tool to provide a valid instant. However, the complexities in controlling the experimental condition became a key issue due to the extreme small scale of nanowires. Exceptional substrate or manipulators are required to measure the response in all situ experiments, which involves nanowires to be subjected to mechanical or electrical excitations. Experimental process faces difficulties in terms of sample fixing, accurate manoeuvring and placement, as well as precise measurement of the force and displacement. While conducting in situ tensile experiments, slight in-plane rotation might occur during the tension process which results in the deflection of the AFM cantilever [14]. Wide applications of in situ experiments are restricted due to unavoidable complexities and uncertainties. By controlling the defects and flaws densities the properties of the nano-wires were reported [12]. Controlling the structures of nanowires by assembling materials in orientated manner some unique properties was demonstrated by [15]. So, to explore the potential applications of

the nano-wires, the knowledge of the influence of different defects on the properties of NWs is important. Furthermore, it is found that many recent experimental studies have appeared as individual study due to various reasons. Firstly, the defects in the nano-scale are difficult to detect. Secondly, having a procedure to recognize the nano-scale fault is not enough, but greater challenge lies in preparing a model with a considered defect for the investigational studies. The in situ experiments can exhibit useful and meaningful information on the properties and performance of nanowires. But in situ experiments basically suffer from various complexities and uncertainties, and the in situ research of the effect on the nanowires properties/performance from different defects is still underdeveloped.

2.5 Numerical studies on nanowires

Due to unavoidable disadvantages of in-situ experiments and progressive demands for investigating the properties of nanowires various numerical and speculative studies have been accepted. Different numerical studies such as molecular dynamics (MD) [16] and multi-scale simulation [17] have been conducted. Especially, the molecular dynamics (MD) simulation is the widely applied method, majority of these are originated from the recent nano-scale experiments. Considering the immense MD studies, this section presents brief details on recent MD simulation studies on different nanowires.

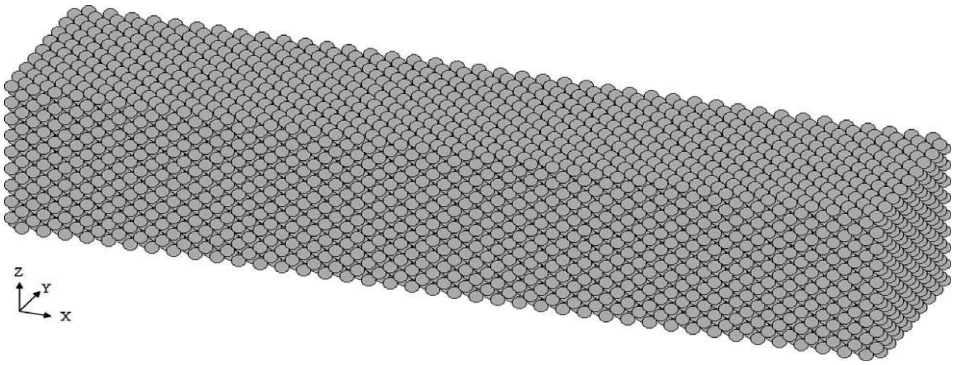

Figure2.8: An initial simulated configuration of Ni nanowire [18].

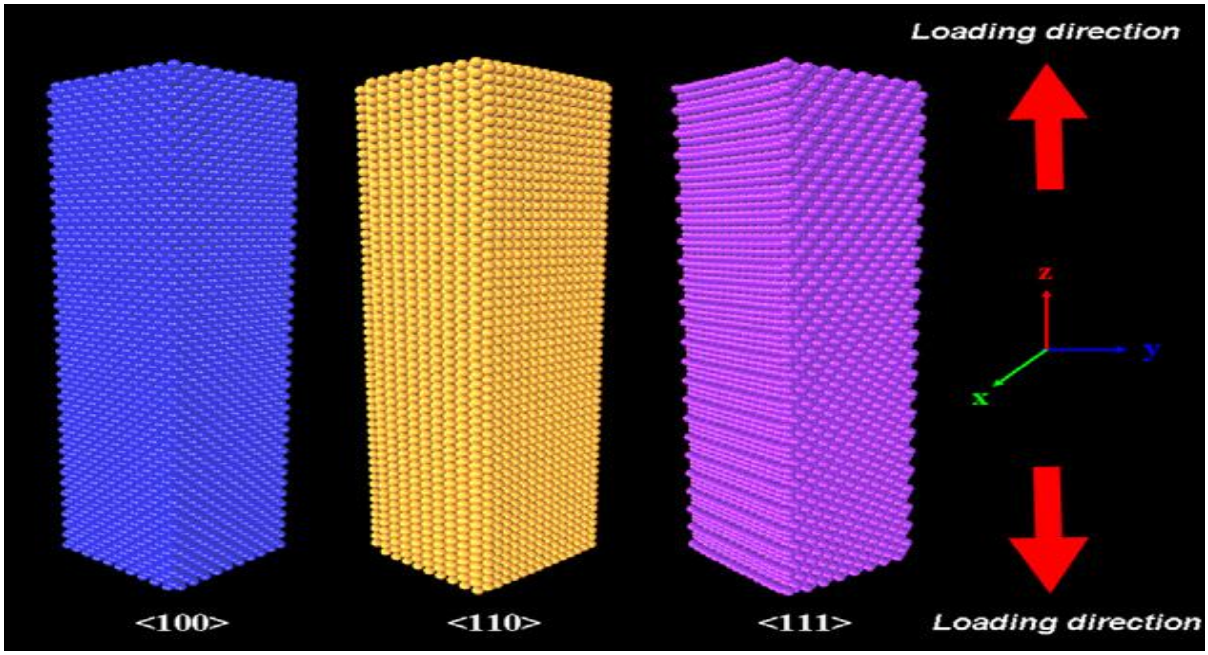

Figure 2.9: Representation of crystallographic direction of three NWs. The loading direction of the Nanowires axis is along the Z direction. [19].

2.6 Tensile simulation

Effortless analysis of tensile stress in the atomistic framework makes MD simulation studies as a suitable candidate for nanowires subjected to axial tension. Tensile properties of diverse nanowires such as the BCC (Fe, Cr and W) nanowires and FCC (Cu, Au, Al and Ni) nanowires have been investigated [20]. Broad significance has been reported for modulus, yield strength and tensile rupture [21]. The consequence of strain rates on the tensile properties of nanowires has been widely investigated based upon, Pt and gold nanowires [22]. According to the large-scale MD simulations conducted on copper nanowires with huge span, short nanowires fails by a yielding form with jagged stress-strain curves, while long nanowires shows tremendous shear confinement and hasty collapse. Mechanical properties for example young's modulus and yield strength of nanowires depends on a range of factors like temperature, loading rate or strain rate, nanowire configuration like nanowire cross-sectional form and crystalline course and nanowire dimension.

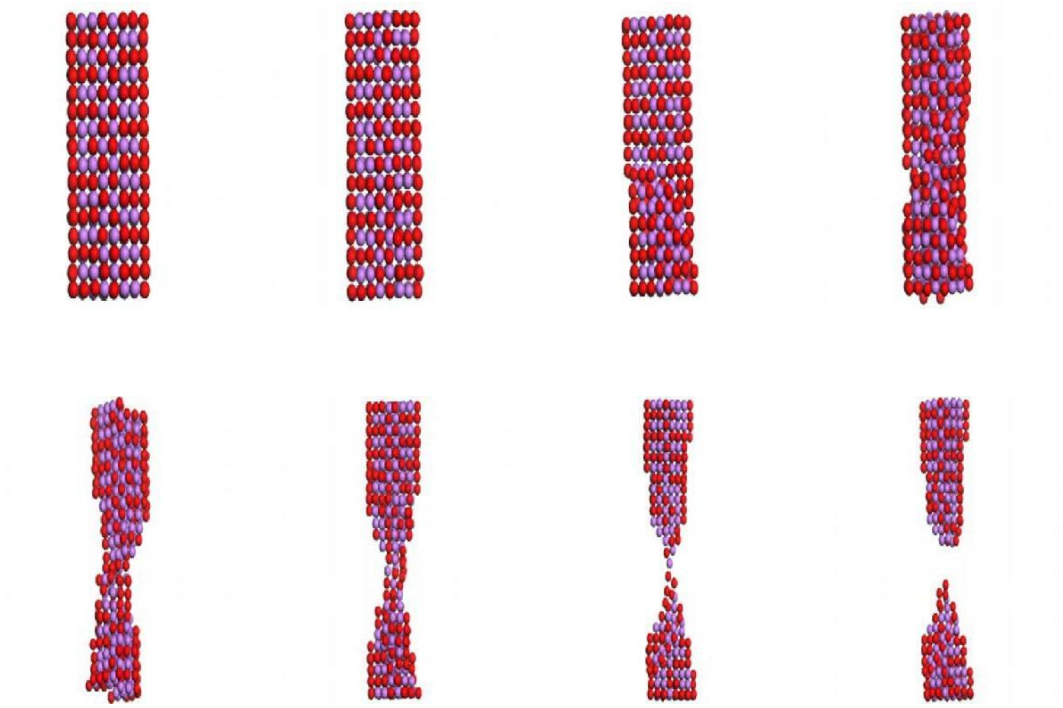

Figure 2.10: Snapshots screened is the atomic orientation of $Pd_{0.5}$-$Pt_{0.5}$ wires at T =300 K and strain rate=0.05% ps^{-1}. Pd atoms are symbolized in red and Pt atoms in purple colour [6].

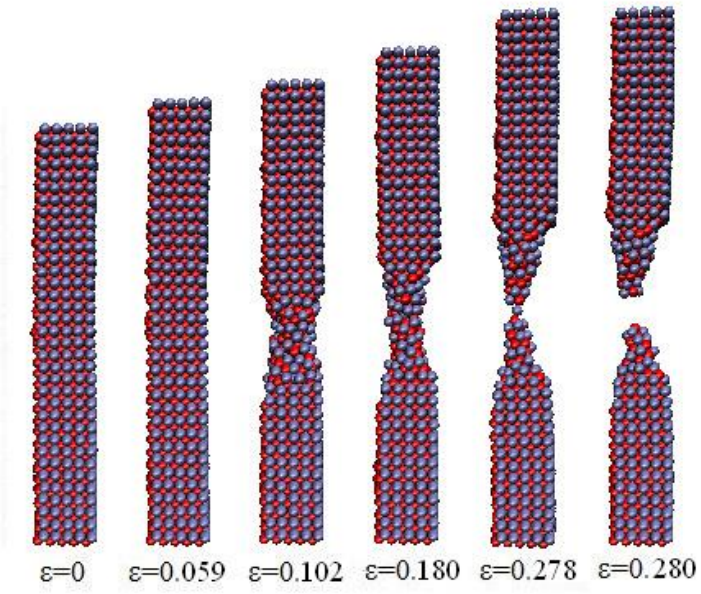

Figure2.11. Snapshots showing atomic arrangement of Ni-Al wires at different strain values for T=300 K and strain rate=0.03% ps-1 [23].

2.7 Applications of nanowires

Nanowires has exciting applications in ample fields, such as the nanocomposites strengtheners [24], the critical part of the solar energy conversion devices, sensors, and the

active components of NEMS, force and pressure sensing, ultrahigh-resolution mass sensing [25] and many more. Expert's findings on nanowires with superior durability, electric conduction, heat conduction, thermal resistance, magnetic properties, and so on. These incredible properties can be summarised as follows:

2.8 Properties of Nanowires

2.8.1 Mechanical properties

Nanowires with FCC crystal structure is a widespread crystal structure for a huge figure of metals and their potentials are well developed, which is essential to perform MD simulations which is widely studied [26] to evaluate the mechanical properties.

2.8.1.1 Effect of temperature

Mechanical properties of the nanowires depend upon simulation temperature has been deliberately studied [26]. Decline of yield strength with growing temperature for a copper nanowire and the reduction can be as much as 77% when temperature ascend from 1 K to 600 K [26]. Low yield strength of metallic nanowires at high temperature is due the thermal variation make possible in overcoming the energy fence for dislocation nucleation.

2.8.1.2 Effect of strain rate

Strain rate is a major factor for evaluating the mechanical properties of the nanowires. The increase in yield strength and yield strains is found to be increase with strain rates using existing computational resources conducted studies in the strain rate range of 10^{7}–10^{11} s^{-1} [27]. The upshot of strain rate on the yield strength of nickel (Ni) nanowire having yield strength value at a strain rate of 108 s^{-1} is established as 7.98 GPa but the yield strength at higher strain rate of 1.4×1011 s^{-1} is established as 11.3 GPa, which is increased by 40% [26]. The reliance of yield stress on the strain rate is supposed to be linked with dynamic wave effects [27], which hinder the initiation of dislocation or occurrence of slip in metallic nanowires. It is seen that the yield strength of nanowire is significantly higher than that of experimental value for bulk nickel (Ni) (i.e. is 0.14 GPa). Due to presence of defects like dislocations, voids and impurities in bulk nickel (Ni), direct comparison of the nanowire with defect free model in MD simulation is not suitable [28]. Nickel nanowires at the highest strain rate were reported as non-linear stress-strain behaviour due to the constrained dynamic free vibration [28]. The yield strength is increased by 23% for higher strain rate of 4×1010 s^{-}

[1]for a platinum (Pt) nanowire. The rise in the yield strain with strain rate pretends a strain hardening mechanism in MNWs [28].

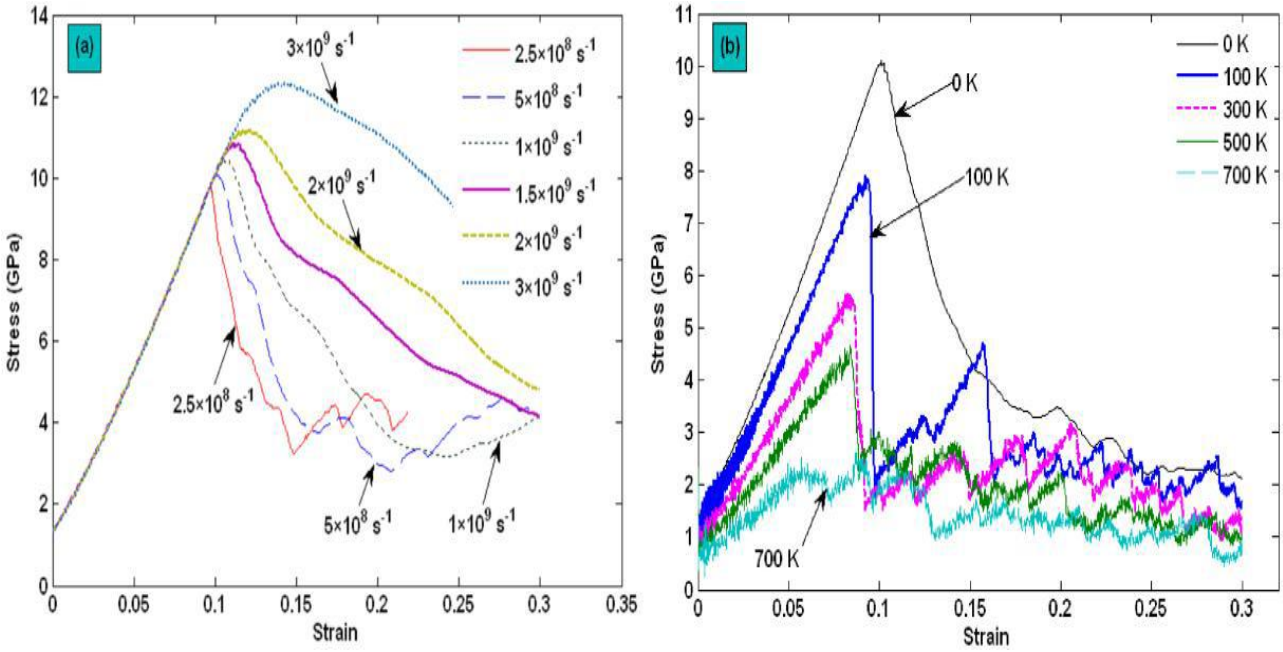

Figure 2.12: Stress-strain curves of a copper nanowire: (a) At different strain rates; (b) At different temperatures [29].

2.8.1.3 Strain Rate Sensitivity

The chief trait of a super plastic material is thought to be the inconsistent elevated sensitivity of the flow stress, σ, to the strain rate, ε. In order to describe this property numerically, one can begin the so-called *strain-rate sensitivity index*, m and *K* is a constant of the material.

$$\sigma = k\epsilon^m$$

The worth of *m* does not habitually go over 0.1 in support of the majority recognized materials. Though, for the materials in a super plastic condition the value of *m* usually lies in the series 0.3 *to* 0.9 and could accomplish around 1,which match up to Newtonian viscous flow. It ought to be noted that the border between super plastic and non-super plastic states for a known material at a set temperature is typically determined experimentally on the foundation of an empirical condition $m \geq 0.3$. Hence the elevated strain rate sensitivity is the mainly vital standard of a super plasticity; consequently the progress of extraordinary means anticipated to estimate this attribute numerically is of concern [30].

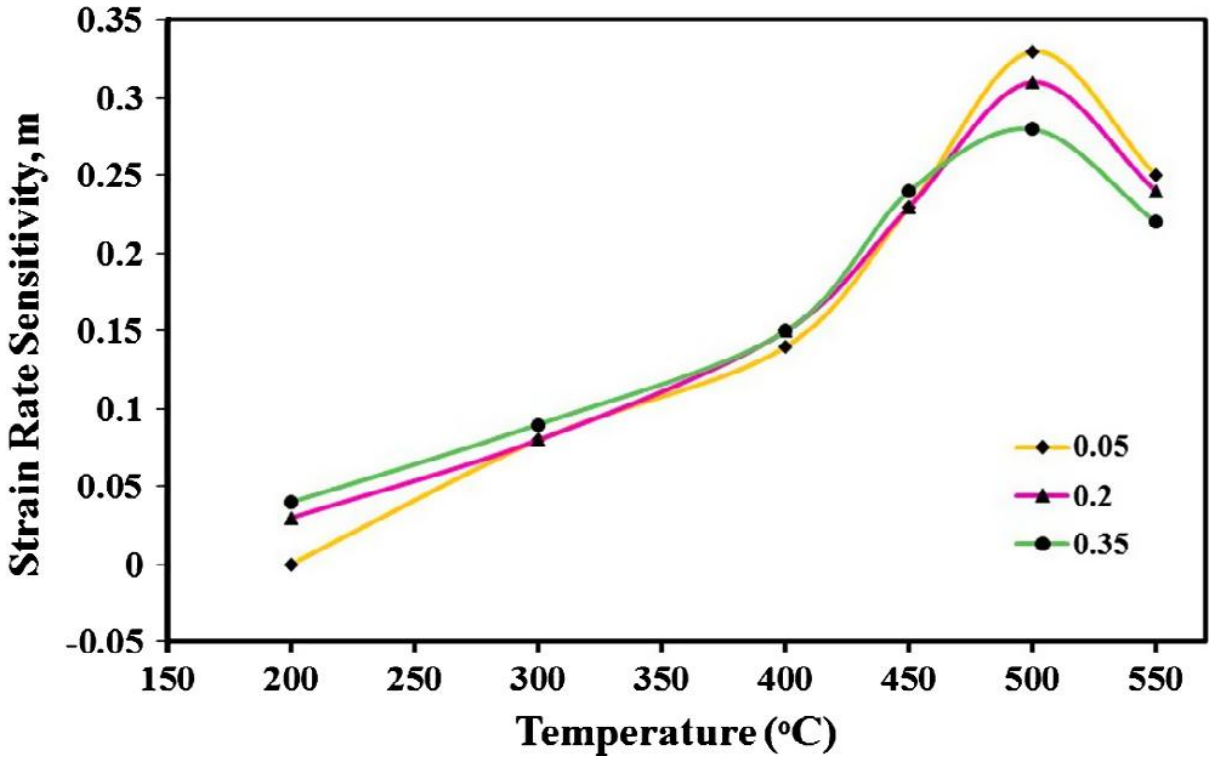

Fig 2.13 The strain rate sensitivity (m) as a function of deformation temperature (at true strains of 0.05, 0.2, and 0.35) [31].

2.8.1.3 Yield strength

Due to computational limitations majority of the existing MD simulations are focused on nanowires with less than 10 nm diameter. The yield strength of metallic nanowires can be hundred times higher than that of corresponding bulk materials [26].

2.8.1.4 Magnetic properties

Nanowires are understood by compact measure of coordination and bonding favour added restricted electronic states and states of higher densities, which encourage genuine magnetic properties. The Pd and Pt nanowires are established as ferromagnetic up to room temperature, which propose future uses in memory-effect-related spintronics [32].

2.8.1.5 Thermoelectric properties

ZT is a thermoelectric material facing challenges in optimizing one physical constraint which unfavourably affects another constraint. Increasing the competence constraint of *ZT*, it has a purpose of the thermoelectric power or See beck coefficient, and of the electrical and thermal conductivities [32].

2.8.1.6 Electrical properties

Numerous future electronic applications of nanowires have been reported in findings by the researchers. Semiconductor nanowires such as Gallium arsenide and gallium phosphate have publicized superior rectifying quality. A number of semiconductor devices such as junction diodes, memory cells and switches, transistors, inverter, and others, have previously been made-up using nanowire junctions [32].

2.8.1.7 Optical properties

Unvarying morphology and appealing optical properties of nanowires have increased their prospective for diverse optical uses. Nanowires prepared by various metal segments like silver, gold, Nickel, Palladium can be applicable as an optical read outs [32].

2.8.1.8 Chemical properties

Nanowire having single crystal quasi-one-dimensional metal oxide has been generally functional in chemical sensing, which reveal momentous improvements on the firmness of the sensors. The growth of nanowire based pH sensor, lead nanowire based hydrogen gas sensor [32] have been reported.

Chapter-3

Computational Method

3. Computational Method

3.1 Motivation

Before coming to MD simulation, it is indispensable to point out diverse simulation techniques used by researchers to explore the possessions of materials. Among them, Finite Element Method, Meshless Method, MD simulation, approaches like first Principal Calculation and multi-scale are the fundamental tools. Mostly, for bulk materials, the methods used are finite Element Method (FEM) and Mesh less Method is used. The First Principal Calculation can only consider tens or a few hundreds of atoms, the multi-scale approaches was developed to study the mechanical properties of nano-materials which is yet limited by the conversion action between diverse approaches like different size range and time range. To bridge the gaps between static simulation and dynamic simulation, MD simulation will be betrothed to get done the motto of the work.

3.2 Molecular dynamics (MD)

Molecular Dynamics technique cause configuration by resolving the classical equations of motion for a body organization with N constituent parts acting together between themselves. Molecular Dynamics is a computer simulation technique using statistical mechanics principle, which is based on the physical movements of atoms and molecules. The material properties show the different approach in the atomic level and the corresponding smallest units. It is also predicted as a virtual microscope with high temporal and spatial resolution. The MD simulations endeavour to forecast the time-dependent route in a system of acting together particles. In MD simulation method statistical assembly averages are equal to time averages of the system. This process of interactions of hard spheres was developed by Alder and Wainwright between 1957 and 1959. Later, the crucial progress for simulating liquid water through molecular dynamics was prepared by Rahman and Stillinger.

3.3 Assumptions

Some basic assumptions must be considered during molecular dynamics simulation. Firstly, the entire molecules and atoms in the simulation are assumed as an arrangement of interacting material points because the nuclei are considered to be much heavier and sluggish than electrons. The motion is explained using its own vector of positions and velocities for each material point. Secondly, due to integration of the classical equations of motion this

study of the development of this system is done for a desired number of time steps. The following steps are followed while molecular dynamics simulation.

- The description of initial positions and velocities of every atom are done.
- The interatomic potentials are used to investigate the forces between these atoms. After a small interval of time the forces are identified, the atomic positions and velocities changes to a second state.
- The repetition of identification of positions and velocities is carried out until the end of the simulation.
- The total energy of the system remains constant because no mass alteration (i.e. No atoms are entering or leaving the simulation box) occurs in the system during the simulation.

3.4 Interatomical potentials

To identify the potential function we need to calculate the forces. Diverse potential approaches were anticipated by researches in the idea of explaining the relationship between different kinds of atoms or molecules, which can be regarded as a pair potential and multiple-body potential. Molecular Dynamic simulations require the definition of an interatomic potential function for describing the interaction with the particles. Potential energy of the structure is represented by the location of the atoms in a specific configuration. It is usually described using the comparative location of the particles with respect to each other, rather than from absolute locations. The general structure is the one following:

$$U(r_1,r_2,...)=V_1+V_2+V_3 \quad \text{.....(3.1)}$$

Gravitational or electrostatic force fields is represented in the first term of this energy equation, but it is ignored, pair-wise interactions of the particles are shown in second term and the third term provides the three-body components but it is incorporated in the second term to diminish the computational outlay of simulation. The other following terms are interactions between more than three bodies and they are usually not considered.

3.4.1 Pair potential

There are different types of pair potential available to portray various atom/molecule interactions, such as Born-Lande potential, which is usually used to describe ion lattice. The Morse potential is an empirical potential that explains the stretching of a chemical bond with its asymmetric pattern which is found to be difficult to compress a bond as compared to pulling a bond apart. It is used to describe solid metal applications such as copper atom.

3.4.2 Multiple-body Potential

Stillinger-Weber multiple-body potential and Tersoff potential are the multiple-body potential which has acquired admired applications due to its accurate interactions between atoms or molecules. Tersoff potential is a three-body potential function that clearly contains an angular involvement of the force, which is extensively applicable for silicon, carbon, Germanium, and others.

3.4.3 EAM method

The embedded atom method (EAM) is a multi-body potential usually used for metallic systems. EAM is an estimate relating the energy between two atoms. It is a sum of functions of the parting among an atom and its neighbours. The EAM function is calculated pragmatically by fitting to the sublimation energy, equilibrium lattice constant, elastic constants, and vacancy-formation energies of the pure metals and the heats of solution of the binary alloys. There are some considerable exertions related with the uses of the pair potentials when the local background is somewhat unlike from the homogeneous mass. This comprises problems like surfaces, grain boundaries, etc. In this argumentation it is considered that every atom is entrenched in a crowd electron gas fashioned by all neighbouring atoms. The quantity of energy requisite to introduce one atom into the electron gas of a specified density is called the embedding function, which considers many-atom effects. In a simulation, the potential energy of an atom, *i*, is given by

$$E_i = F_{\propto}\left(\sum_{i\neq j}\rho_{\beta}\left(r_{ij}\right) + \frac{1}{2}\sum_{i\neq j}\varphi_{\alpha\beta}\left(r_{ij}\right)\right) \quad \text{.....(3.2)}$$

Where *rij* is the distance between atoms *i* and *j*, ϕ_{ij} is a pair-wise potential function, ρ_β is the electron charge density from atom *j* of type β at the location of atom *i*, and *F* is an embedding function that represents the energy required to place atom *i* of type α into the electron cloud. The geometric mean is specified for the interaction between a pair of species which is repulsive in nature. For a sole element organization of atoms, three specified role are scalar. The entrenched function, a pair-wise communication, and an electron cloud role function. For a binary alloy, the EAM potential needs seven functions: three pair-wise interactions (A-A, A-B, B-B), two set in functions, one for each type of atom, and two electron cloud contribution functions This mode has been functional for learning fracture and defects, grain boundaries and erstwhile metallic systems and methods.

3.5 Equations of motion

The simulations carried out by molecular dynamics method are based on solving the classical equations of motion for an *N* body system interacting through a potential function *V(r1, ..,rN)*. These equations of motion are then given by Newton's laws:

$$m_i \ \frac{d^2y}{dx^2} = F_i \text{.....(3.3)}$$

Where, F_i is the force of i^{th} particle which is derived from,

$$F_i = -\nabla_i v(r_i, \ldots . r_n) \text{.....(3.4)}$$

3.6 Integration

Forces should be integrated for the mobility of atoms in a molecular dynamics simulation. Millions of atoms are considered in molecular dynamic simulations; it is very tedious and difficult to analyse a system amid such a huge figure of atoms. Hence, a system is applied to a numerical integration method. Familiar numerical integration techniques comprise of Verlet algorithm, leap-frog algorithm, Velocity-Verlet, and Beeman's algorithm. The molecular dynamics software used in our study Verlet integration method.

3.6.1 Time integration algorithm

Time integration algorithms are relied on finite difference methods. Here time is discretized with a time step **Δ***t* that is the distance between consecutive points on the grid created. The integration scheme gives the location and some of their time derivates at a certain time *t* + **Δ***t*

once those quantities are known on the previous time *t*. The time progress of the system can be trailed by iterating this procedure.

3.6.2 The Verlet algorithm

The generally used time integration algorithm in molecular dynamics simulation is the Verlet algorithm. This contains two Taylor expansions for positions *r(t)*, one presumptuous and the other hesitant in time. Third order ranges are going to be the velocities, *v(t)*; the accelerations, *a(t)*; and third order derivates of the position *b(t)*.

$$r(t-\Delta t) = r(t) - v(t)\Delta t + \frac{1}{2}a(t)\Delta t^2 - \frac{1}{6}b(t)\Delta t^3 + O(\Delta t^4) \quad \text{.....(3.5)}$$

$$r(t+\Delta t) = r(t) + v(t)\Delta t + \frac{1}{2}a(t)\Delta t^2 + \frac{1}{6}b(t)\Delta t^3 + O(\Delta t^4) \quad \text{.....(3.6)}$$

By adding the above expressions the following equation is derived and is the fundamental form of the Verlet algorithm.

$$r(t+\Delta t) = 2r(t) - r(t-\Delta t) + a(t)\Delta t^2 + O(\Delta t^4) \quad \text{.....(3.7)}$$

Due to the simplicity in terms of implementation, accuracy and stability; verlet algorithm is widely used tool in molecular dynamics simulation technique. Based on the accelerations obtained from the new forces, the simulation proceeds by iterative calculation of forces and solving the equations of motion is done. This is typically the largely useful test to validate that a MD simulation is scheduled precisely.

3.7 How a simulation runs

Initially, in a Molecular Dynamic simulation, we simulate the label of the system. This explains that the atoms initial position and dimensions have to be well-known. Then elements are defined and a potential function is selected a time step has to be chosen. Establishing the forces between the atoms of the system is being simulated and the time integration algorithm is being used to work out the equations of motion. The new positions of atoms are configured through simulation by allocating itself in the new position. This corresponds to one time step ahead when continued with simulations and is continued till a specific condition is reached through simulation after a specific number of time steps. On the other hand, round-off errors

decrease slower than the truncation ones with a declining **Δ***t* and dominate in the small **Δ***t* limit.

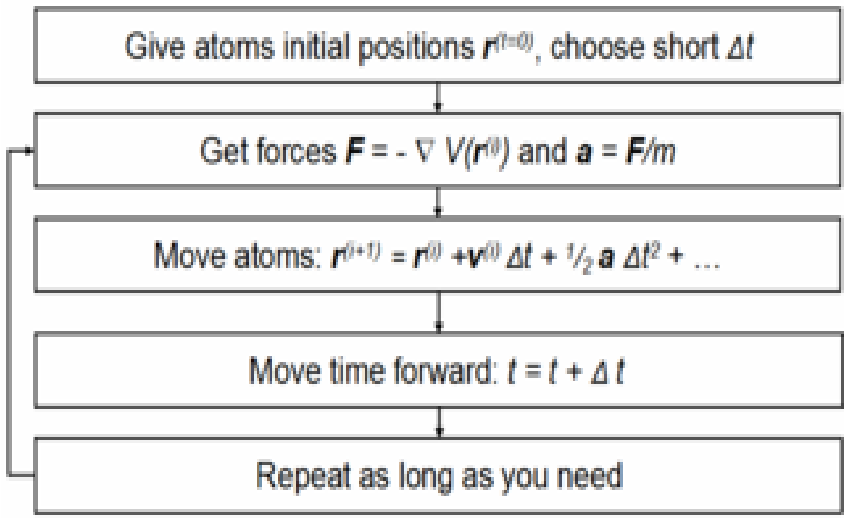

Figure 3.1: Simulation hierarchy flowchart [33]

3.8 Ensembles

Some theoretical tools are used to study its effect on simulation. Time averages are correspondent to the ensemble averages are the major consideration for evaluating the simulation results. The need of statistical ensemble is to know the tool composed of descriptions of probable micro-states. Accumulation of micro-states tends to the same properties in the macro-state. Basically, MD simulation is carried out under definite equilibrium ensembles. Some frequently used ensembles as listed below

NVE ensemble: It is used to examine an isolated thermodynamics system. In this ensemble, the particles (atoms or molecules) number (N), volume (V) and energy (E) of the simulation system remains constant.

NVT ensemble: It is used to describe a probability distribution of microscopic states of the system. Here, the particles number (N), volume (V) and temperature (T) of the simulation system uphold constant.

NPT ensemble: It is also known as isothermal-isobaric ensemble. Here, the particles number (N), pressure (P) and temperature (T) of the simulation system hold constant.

NPH ensemble: It is also called as isoenthalpic-isobaric ensemble. Here, the particles number (N), pressure (P) and enthalpy (H) of the simulation system are kept constant.

3.9 Simulation drawbacks

Some limitations have to be taken into description in the form of forces calculations which come out while simulating bulk atoms. The relative positions of these atoms travel under the feat of the instantaneous forces and thus their relative position and the forces also changes. The accuracy in simulation will be exhibited only if the interatomic forces are realistic and these forces are found as the ascent of a potential energy function. The role of potential chosen is vital to evaluate the behaviour of the material.

3.9.1 Time and size limitations

The simulation of large number of atoms in an instant of time with large space time resolution is performed in MD simulation. The factor like time step is crucial in determining the duration of simulation and is done in two steps for finding the correct time. Initially, an appropriate time step (i.e. small enough) is chosen to view a realistic continuous atomic movement. Secondly, the time step ought to be outsized to cut off the duration of simulation. To get better efficiency of the simulation; non constant time step is chosen when the velocity is deviated during simulation.

3.9.2 Boundary conditions

For running MD simulation, the choice for the boundary condition (BC) is very vital. Due to the limitations in computer efficiency; Molecular Dynamic simulation can provide a small group of atoms of the system under analysis. In general, periodic, non-periodic boundary conditions or the permutation of the two is chosen. Periodic boundary condition explains infinite size that obstructs the free boundary effect. Hence, periodic boundary conditions are typically obligatory to rise above those problems. However, non-periodic boundary condition is functional to study the non-equilibrium system, but always induce a free boundary effects. So, selecting the correct BC for a simulation is a decisive and intricate work.

3.10 LAMMPS

LAMMPS is an open-source project distributed by Sandia National Laboratories which is abbreviated as Large-scale Atomic/Molecular Massively Parallel Simulator. is run on a single processor or run in parallel utilizing message-passing parallelism (MPI). While running in parallel it spatially fester the system. It is written in C++ which allows it to be highly portable. It is assembled and run on a large number of machines and operating systems.

About an input script of LAMMPS:

LAMMPS is carried out by accessing input script (text file) commands. Every command grounds LAMMPS to take some action and it exits when the input script ends. It sets an internal variable, read in a file, or run a simulation. The majority of commands have default settings, which can be changed upon once requirements.

The structure of an input script in LAMMPS is the one that follows:

1. Initialization
2. Atom and Lattice description
3. Force fields
4. Settings
5. Run

The following commands describe the input script for creating a Pd_{50}-Pt_{50} alloy nanowire.

Initialization

Definitions of the units that are going to be used during the simulation i.e. metal units are: distance = Å, time = picoseconds, energy = eV, velocity = Å/ps, temperature = K, pressure = bar.

```
units           metal
echo            both
```

The boundary conditions that are employed in LAMMPS are:

ppp; p p s; p f p

Where ‘p’ stands for periodic along the three directions, ‘f’ and‘s’ stand for fixed and

shrink wrapped, which are non-periodic.

boundary p pp

Definition of the simulation dimensions, in this case 3D.

dimension 3

Atom and Lattice definition

The atomic type is the one that matches better with metals simulation.

atom_style atomic

region my cylinder y 0 0 10 0 100 units box

create_box 2 my

Definition of the type of lattice

lattice fcc 3.89

Definition the region that is going to be studied

region mine cylinder y 0 0 10 0 100 units box

create_atoms 1 region mine units box

lattice fcc 3.89 orient x 1 0 0 orient y 0 1 0 orient z 0 0 1

Force field

Set region my type/fraction 2 0.5 12393

Choice of the interatomical potential that is going to be used and the directory to find the parameters. The "*" indicates that the potential is going to be applied between all the types of atoms defined.

pair_style eam/alloy

pair_coeff * * PdPt.set Pd Pt (force field parameter)

Setting

LAMMPS performs an energy minimization of the system, by iteratively regulating atom coordinates. The minimizers hurdle the far away atoms movement in single iteration, so that it is possible to slow down systems with exceedingly overlie atoms (huge energies and forces) by approaching the atoms off each other.

minimize	1.0e-6 1.0e-5 100 100(energy minimization)

Definition of the frequency with which the output information is going to be registered and which variables are going to be recorded.

thermo	10 (output)
thermo_style	custom step temp etotal pyy

The output of the LAMMPS simulation is written onto text files called dump file containing the information of the atom coordinates along with the velocities dumped at the required timestep. While the thermodynamic information of the simulation is stored in as log file.

dump	1 all custom 10 pd-pt_wire_dump.lammpstrj id type x y z (output)
log	log pd-pt wire.data

Give some initial velocity to all the atoms randomly

velocity	all create 100 45875 rot yes mom yes dist Gaussian

Run the simulation

fix	1 all npt temp 100 100 0.1 iso 0 0 0.1
timestep	0.002
run	100
unfix	1

The following input file depicts the tensile sample for Pd_{50}-Pt_{50} alloy nanowire:

Initialization

units	metal
echo	both
atom_style	atomic
dimension	3
boundary	p pp

Atom and Lattice definition

read_data	sample_data_tensile.txt
timestep	0.002

```
compute         1 all stress/atom
compute         2 all reduce sum c_1[1] c_1[2] c_1[3]
variable        stress equal ((c_2[2])/(3*vol*10000))
variable        tmp equal ly
variable        lo equal ${tmp}
variable        strain equal (ly-v_lo)/v_lo
variable        p equal -pyy/10000
thermo          100
thermo_style    custom step temp vol etotal pyy lx ly lz v_stressv_strain
```

Force field

```
pair_style      eam/alloy
pair_coeff      * * PdPt.set Pd Pt
```

Setting

```
dump            1 all custom 100 NVT_defo_dump_100K.lammpstrj id type x  y z
log             NVTlogdefpdpt_100K.data
velocity        all create 100 873847 rot yes mom yes dist gaussian
```

Run the simulation

```
fix             2 all deform 1 x volume y trate 0.01 z volume units box
fix             1 all nvt temp 100 100 0.1
run             75000
```

3.11 Visual Molecular dynamics (VMD)

VMD is a molecular visualization package for exhibiting, animating, and evaluating large atoms/molecules using 3-D graphics and built-in scripting. In the present study all the atomic snapshots are taken by VMD software (Humphrey et al., 1996).

Chapter-4

Results & Discussions

4. Results and Discussion

4.1 Platinum nanowire

4.1.1 Stress-Strain plot

The simulation inferences from the MD simulation are accessible from the following Figure4.1.It shows the stress-strain association of the Pt-nanowire, replicated at 100 K, 300 K, 500 K, and 700 K each for strain rates of 1%, 3%, 5%, 8% and 10% ps^{-1}, respectively. The mechanical properties of Pt nanowire are strongly dependent on the investigated temperature and strain rate constraints. The outcome of these constraints on Young's modulus, yield stress was investigated independently in the subsequent segments.

It is seen that, ahead of the elastic area, the stress slump rapidly soon after the yield point has reached. The strain rate exhibits a notable control on the stress–strain activities. For low strain rates, the stress–strain relations show a lucid crisscross curve as the strain is increased. The stress ascends, and then fall in a repeating fashion. The fracture takes place before 50% strain; lower fracture strain corresponds to lower strain value. The stress–strain relations exhibits an unlike nature for higher strain rates. We are not able to observe the discrete fall/elevate cycle in stress as the strain increases.

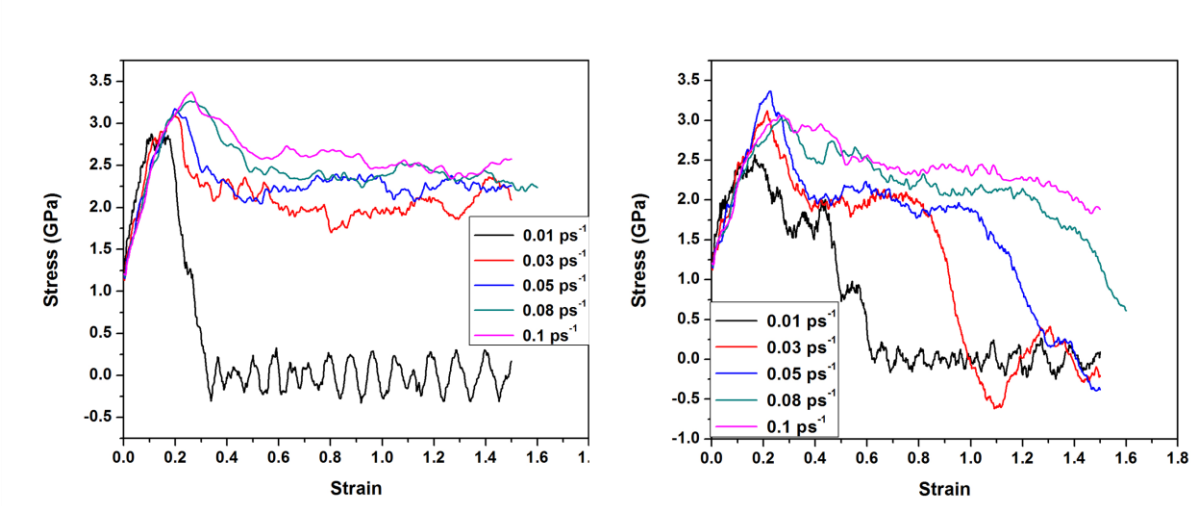

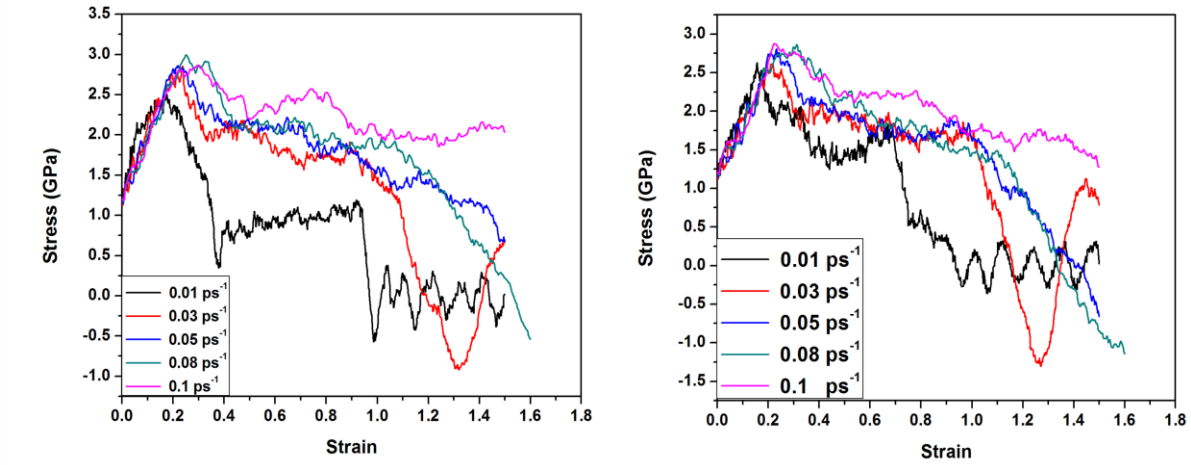

Fig. 4.1 Stress-Strain plot of Pt nanowire deformed at (a) 100 K (b) 300 K (c) 500 K (d) 700 K temperatures. Each sample is deformed at the strain rate ranging from 1% to 10% ps^{-1}.

4.1.2 VMD snapshots

The visual molecular dynamics (VMD) software is used to visualize the activities carried out in molecular dynamics simulations. Its equivalent atomic arrangements were revealed in Fig.4.2, in different strain conditions. We observe that at strain value 0, the Pt nanowire is in perfect crystalline form. Subsequently, with the increase in strain values the nanowire deforms and at the strain value 0.34 the necking phenomenon is observed which corresponds to ductility and fracture occurs at the strain value of 0.46.

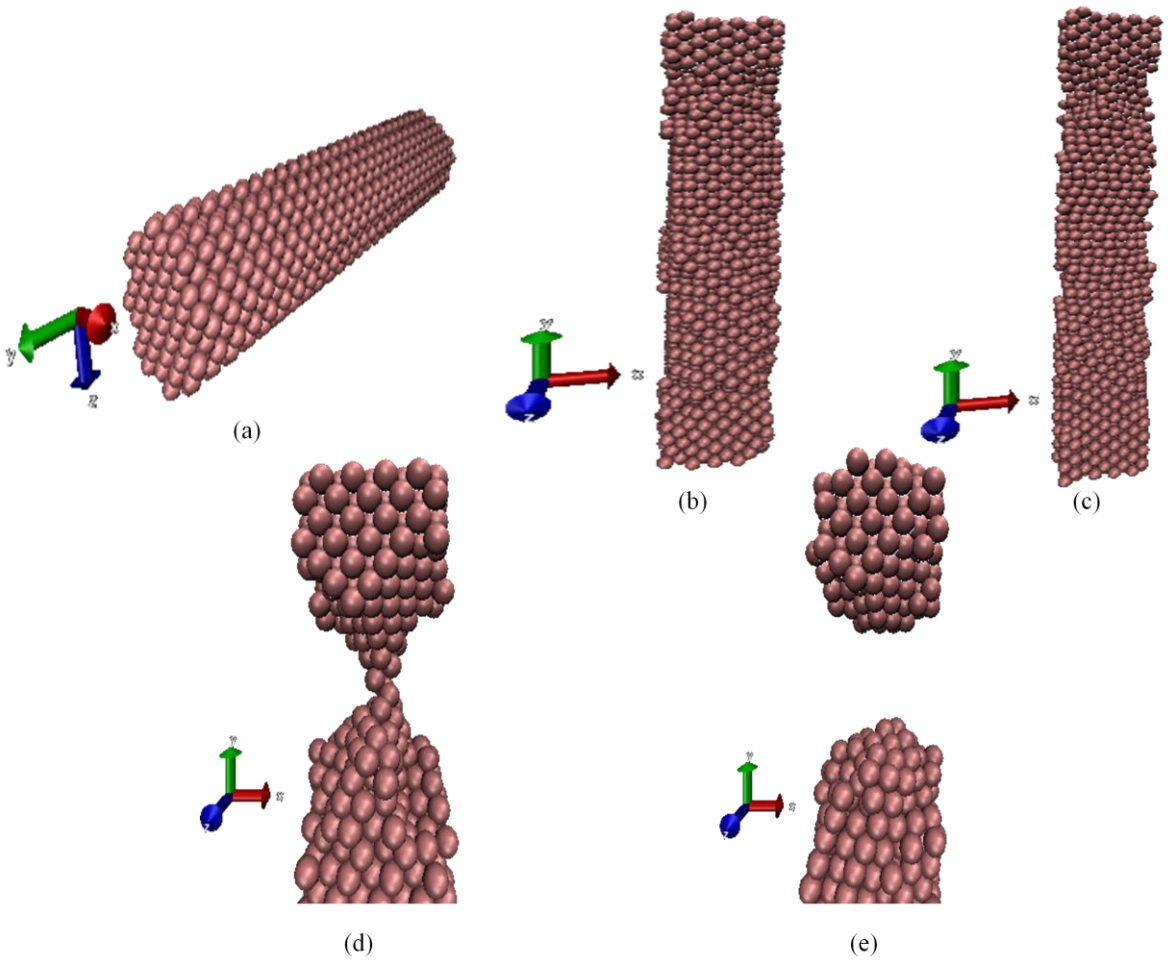

Fig.4.2. VMD snapshots of Pt nanowire at different strains (strain rate= 0.01 ps^{-1} and 100 K temperature): (a) 0 (b) 0.1 (c) 0.26 (d) 0.34 (e) 0.46.

4.1.3 Yield Strength variation

A representation of Pt-nanowire with circular cross sections is shown in Figure 4.2. MD simulation results focused on the effect on yield strength due to the variation in strain rate and temperature is discussed in the following sections.

4.1.3.1 Effect of Strain Rate

To examine the control of strain rate, we deform the same sample using diverse strain rates in the range of 1% to 10% ps^{-1} strain rate. The effect of strain rate on the yield strength of Pt nanowire is depicted in Figure 4.3(a). The yield strength value at a strain rate of 1% ps^{-1} and 100 K temperature condition is found to be 2.04 GPa but the yield strength at higher strain rate of 10% ps^{-1} is found to be 2.42 GPa. The values mentioned in Table 4.1. is observed to be fluctuating but the trend is increasing in nature it is also noted that yield stress increases and fluctuates with strain rate in a non-linear manner. The reliance of yield stress on the

strain rate is understood to be related with a dynamic wave effect [26], which hinders the dislocation commencement or happening of slip in nanowires. The strain rate taken up here is very elevated match up to that in experiment, since the molecular dynamics time scale located by the atomic movement is extremely short in terms of time.

4.1.3.2 Effect of Temperature

To explore the influence of temperature, we distort the same sample using diverse temperature in the range of 100K to 700K. The basic trend shown in Fig.4.2 (b) depicts that the yield strength decreases with increasing temperature from 100 K to 700 K for Pt nanowire. Low yield strength of Pt nanowire at high temperature is because of the fact that the thermal fluctuations make possible to rise above the energy obstruction for dislocation nucleation. But we see some fluctuations in the trend due to the creep deformation which largely contribute to the strength decline at higher temperature. Each curve is different at each temperature and increases as well as decreases with increasing temperature. At minor test temperature and elevated strain rate, the creep deformation is accepted to be smaller.

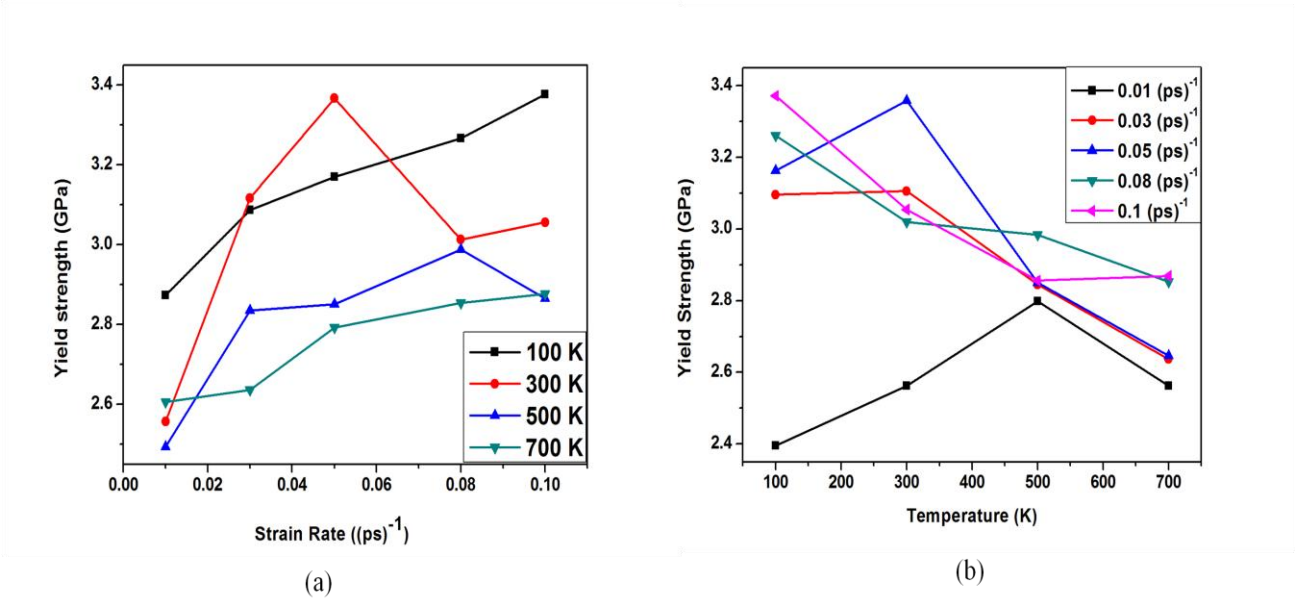

Fig.4.3. Variation of yield strength of Pt nanowire: (a) Strain rates (b) Temperature.

Table 4.1 Yield strength variation w.r.t Strain rate for Pt nanowire

Strain Rate (ps^{-1})	**Yield Strength (100K) (GPa)**	**Yield Strength (300K) (GPa)**	**Yield Strength (500K) (GPa)**	**Yield Strength (700K) (GPa)**
0.01	2.39	2.56	2.79	2.56
0.03	3.09	3.10	2.84	2.63
0.05	3.16	3.35	2.85	2.80
0.08	3.26	3.01	2.98	2.85
0.1	3.37	3.05	2.85	2.86

Table 4.2 Yield strength variation w.r.t Temperature for Pt nanowire

Temperature (K)	**Yield Strength ($0.01ps^{-1}$) (GPa)**	**Yield Strength ($0.03ps^{-1}$) (GPa)**	**Yield Strength ($0.05ps^{-1}$) (GPa)**	**Yield Strength ($0.08ps^{-1}$) (GPa)**	**Yield Strength ($0.1ps^{-1}$) (GPa)**
100K	2.39	3.09	3.16	3.26	3.37
300K	2.56	3.10	3.35	3.01	3.05
500K	2.79	2.84	2.85	2.98	2.85
700K	2.56	2.63	2.80	2.85	2.86

4.1.4 Elastic Modulus variation

The effect of temperature and strain rate on the elastic constant is shown in Figure 4.4 and discussed in the following section.

4.1.4.1 Effect of strain rate

In Fig. 4.4 (a), we observe that, at low strain rate and low temperature the modulus value is high as compared to that of high temperature and low strain rate condition but in case of 500 K temperature condition the elastic modulus value is observed as high, which is against the

trend obtained, the cause for this effect is under investigation. The values of elastic modulus at different strain rate conditions are mentioned in Table 4.3.

4.1.4.2 Effect of Temperature

In Fig.4.4 (b), we observe a decreasing trend in Pt nanowire. We see that, at elevated strain rate and low temperature the elastic modulus value is lower and subsequently the elastic modulus values increases with decrease in strain rates. But the trend is observed to be decreasing with the increase in temperature due to relative softening of Pt nanowire. Softening results in reducing stiffness, this corresponds to lower elastic modulus values. The values of elastic modulus w.r.t mentioned temperatures are shown in Table 4.4.

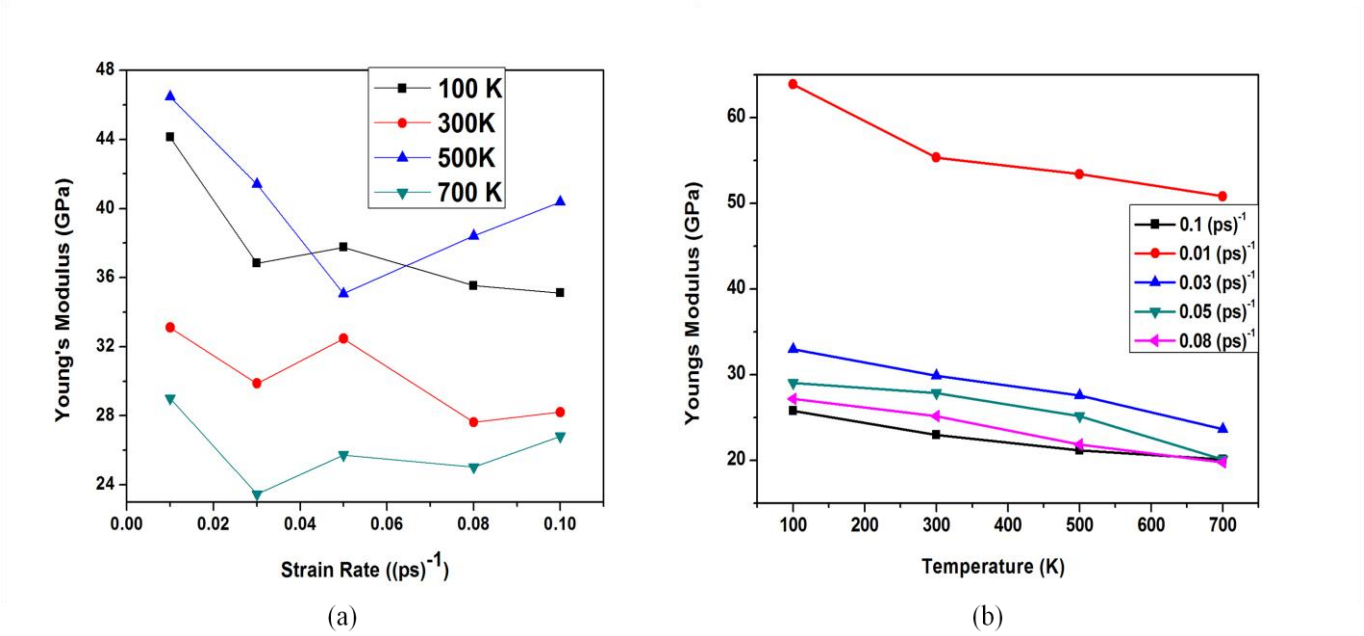

Fig.4.4.Variation of Young's modulus of Pt nanowire: (a) Strain rates (b) Temperature.

Table 4.3 Young's modulus variation w.r.t Strain rate for Pt nanowire

Strain Rate (ps^{-1})	E (100K) (GPa)	E (300K) (GPa)	E (500K) (GPa)	E (700K) (GPa)
0.01	63.87	55.33	53.39	50.80
0.03	32.94	29.87	27.58	23.62
0.05	29.05	27.83	25.14	20.11
0.08	27.16	25.17	21.86	19.78
0.1	25.77	22.97	21.16	20.11

Table 4.4 Young's modulus variation w.r.t temperature for Pt nanowire

Temperature (K)	E ($0.01ps^{-1}$) (GPa)	E ($0.03ps^{-1}$) (GPa)	E ($0.05ps^{-1}$) (GPa)	E ($0.08ps^{-1}$) (GPa)	E ($0.1ps^{-1}$) (GPa)
100K	44.11	36.82	37.75	35.52	35.1
300K	33.11	29.87	32.46	27.62	28.20
500K	46.45	41.40	35.06	38.40	40.37
700K	29.01	23.46	25.73	25.02	26.80

4.1.5 Strain rate sensitivity variation plot

In Fig 4.5, we see a log-log plot of stress vs strain rate and strain rate sensitivity (m) variations w.r.t temperature. The variation of m is quite uneven w.r.t the temperature variations. In Fig 4.5 (a) the flow stress value increases w.r.t strain rate. In Fig 4.5 (b) we observe the variations in the 'm' values due to nano-scale twinning effect. In Pt nanowire the rate-controlling deformation means match up to the release of dislocations from free surfaces is opposed by the transmitted dislocations through coherent twin boundaries [34].

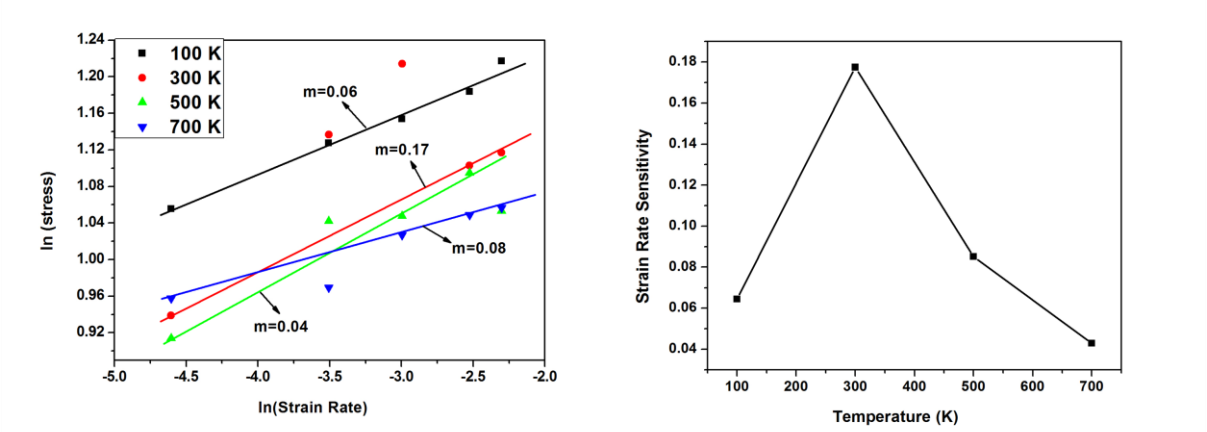

Fig 4.5. Plots for strain rate sensitivity of Pt nanowire (a) ln(stress) vs ln(strain rate) (b) m vs Temperature.

Table 4.5 Strain rate sensitivity variation w.r.t temperature for Pt nanowire

Temperature (K)	Strain Rate Sensitivity
100	0.06
300	0.17
500	0.08
700	0.04

4.2 Palladium (Pd)

4.2.1 Stress-Strain Plot

Figure 4.6 shows the stress-strain association of the Pd-nanowire, simulated at 100 K, 300 K, 500 K, and 700 K each deformed at the strain rates of 1%, 3%, 5%, 8% and 10% ps−1, respectively. It is seen that the mechanical properties like yield strength, young's modulus of Pd nanowire are strongly reliant on the investigated temperature and strain rate constraints [26]. The stress-strain response is almost same as compared to Pd nanowire with some variations in the values of yield strength and young's modulus.

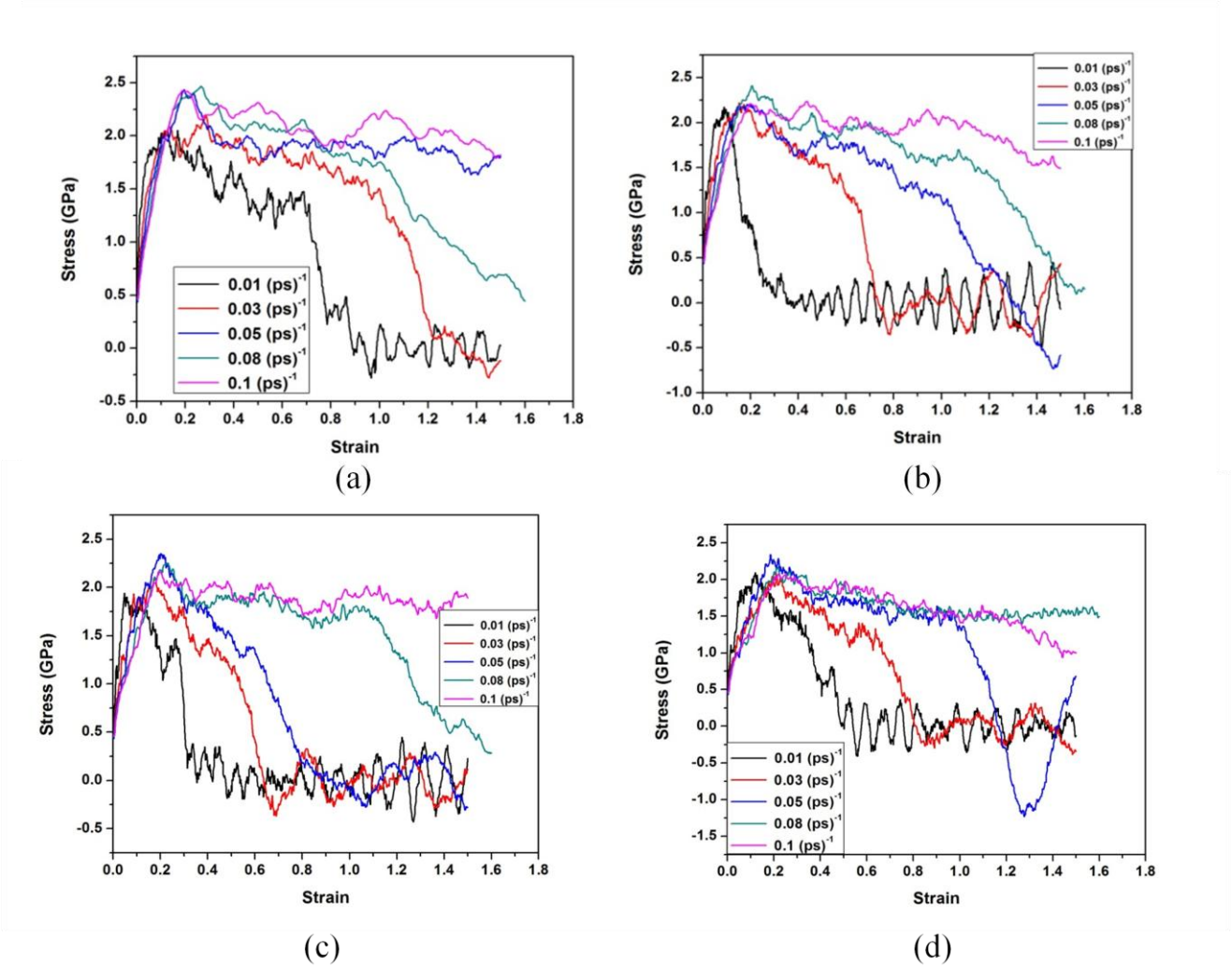

Fig. 4.6 Stress-Strain plot of Pd nanowire deformed at (a) 100 K (b) 300 K (c) 500 K (d) 700 K temperatures. Each sample is deformed at the strain rate ranging from 1% to 10% ps^{-1}.

4.2.2 VMD Snapshots

The visual molecular dynamics VMD software is helpful in visualizing the activities of molecular dynamics simulations. The equivalent atomic activities were shown in Fig.4.2, in different strain conditions. We observe that at strain value 0, the Pd nanowire is in perfect crystalline form. Subsequently, with the increase in strain values the nanowire deforms and at the strain value 0.796 the necking phenomenon is observed which corresponds to ductility. Fracture occurs at the strain value of 0.896.

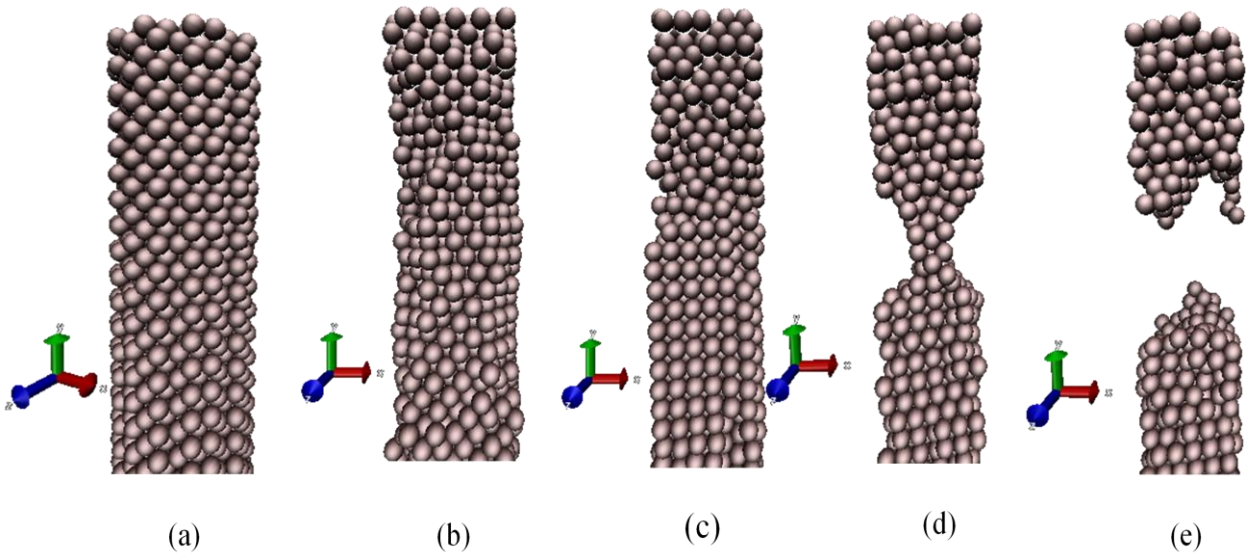

Fig.4.7. VMD snapshots of Pd nanowire at different strain condition (strain rate= 0.01 ps^{-1} and 100 K temperature) (a) 0 (b) 0.2 (c) 0.6 (d) 0.796 (e) 0.896.

4.2.3 Yield Strength variation

A representation of Pd-nanowire with circular cross sections is shown in Figure.4.3. MD simulation results focused on the effect of yield strength due to the variation in strain rate and temperature is discussed in the following segments.

4.2.3.1 Effect of strain rate

In Fig.4.8 (a), we observe that at higher temperature condition and high strain rate value the yield strength is lower and the value of yield strength increases with subsequent decrease in temperature, deformed at same strain rate (10% ps^{-1}). The trend seen in the figure is quite fluctuating due to nanowire initial inequilibrium condition. Conventionally, the trend is

ascending in nature with the decrease in temperature. The detailed values are depicted in Table 4.6.

4.2.3.2 Effect of Temperature

In Fig 4.8 (b), we see that at lower temperature and strain rate condition the value of yield strength is low. With the raise in strain rate the value of yield strength increases. The trend shown in the Figure 4.8 (b) is decreasing in nature with some fluctuations at some conditions. Conventionally, the trend should be decreasing; however, the figure mentioned can be summarised as a decreasing trend. This phenomenon can be justified by the dislocation movement and hindrance w.r.t variation in temperature. With the increase in temperature the barrier for dislocations is erased and the movement is quite mobile and the plastic deformation is carried out easily. The detailed values are depicted in Table 4.7.

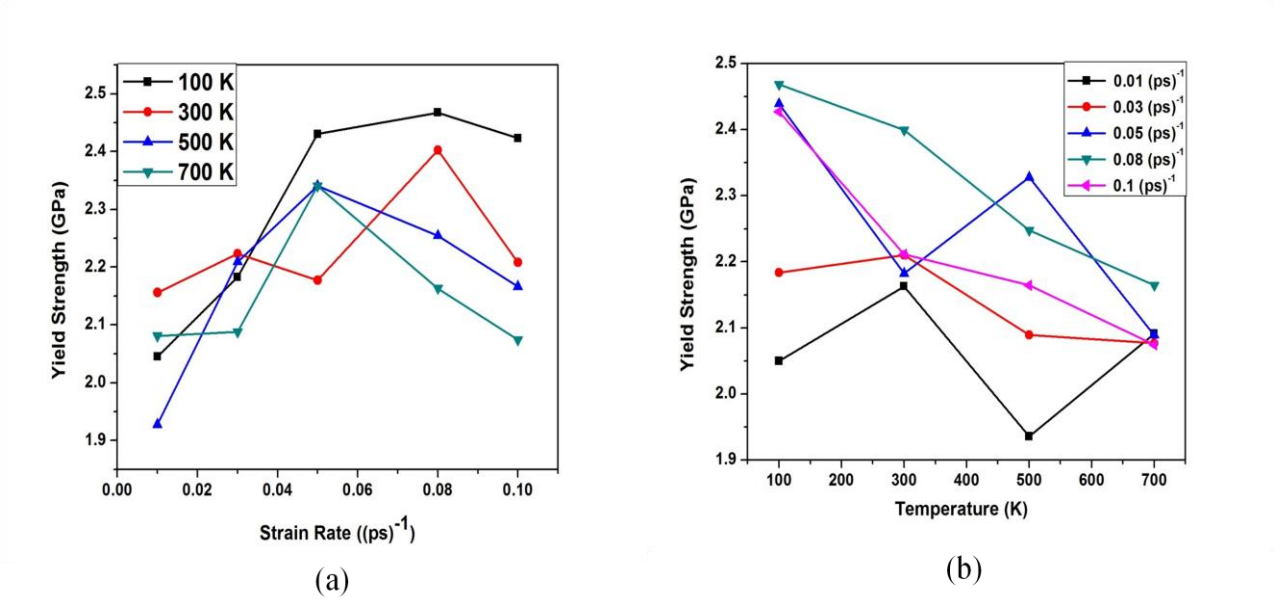

Fig.4.8. Variation of yield Strength of Pd nanowire: (a) Strain rate (b) Temperature.

Table 4.6 Yield strength variation w.r.t Strain rate for Pd nanowire

Strain Rate (ps^{-1})	**Yield Strength (100K) (GPa)**	**Yield Strength (300K) (GPa)**	**Yield Strength (500K) (GPa)**	**Yield Strength (700K) (GPa)**
0.01	2.04	2.15	1.92	2.08
0.03	2.18	2.22	2.20	2.08
0.05	2.43	2.17	2.34	2.34
0.08	2.46	2.40	2.25	2.16
0.1	2.42	2.20	2.16	2.07

Table.4.7. Yield strength variation w.r.t temperature for Pd nanowire

Temperature (K)	**Yield Strength (0.01 ps^{-1}) (Gpa)**	**Yield Strength (0.03 ps^{-1}) (Gpa)**	**Yield Strength (0.05 ps^{-1}) (Gpa)**	**Yield Strength (0.08 ps^{-1}) (Gpa)**	**Yield Strength (0.1ps^{-1}) (Gpa)**
100K	2.04	2.18	2.43	2.46	2.42
300K	2.16	2.21	2.18	2.39	2.21
500K	1.93	2.08	2.32	2.24	2.16
700K	2.09	2.07	2.33	2.16	2.07

4.2.4 Elastic Modulus variation

The young's modulus (E) in the stress-strain curve is calculated by the slope between the origin and a point of the elastic section. MD simulation results focused on the effect of 'E' due to the variation in strain rate and temperature is discussed in the following sections.

4.2.4.1Effect of Strain Rate

The effect of strain rate on 'E' is obtained by plotting the graph of E vs strain rate as shown in Fig.4.9 (a). Roughly the plot exhibits straight lines with even slope for any given temperature with decreasing trend. At lower strain rate and lower temperature the value of elastic modulus is high. Subsequently, it decreases with increase in temperature condition. But, in case of 500 K temperature condition; the trend is quite unlike. The cause for this behaviour is still under investigation. Conventionally, the trend is quite justified; lower temperature makes a nanowire quite stiff which corresponds to higher elastic modulus [35]. The detailed values are depicted in Table 4.8.

4.2.4.2 Effect of Temperature

In Fig4.9 (b), we clearly observe the declining trend with the increase in temperature. At lower strain rate and low temperature condition the value of elastic modulus is quite high and reduces with the increase in strain rate at the same temperature condition. The trend observed in the figure is justified conventionally using softening and stiffness phenomenon as described above for Pt nanowire. The detailed values are depicted in Table 4.9.

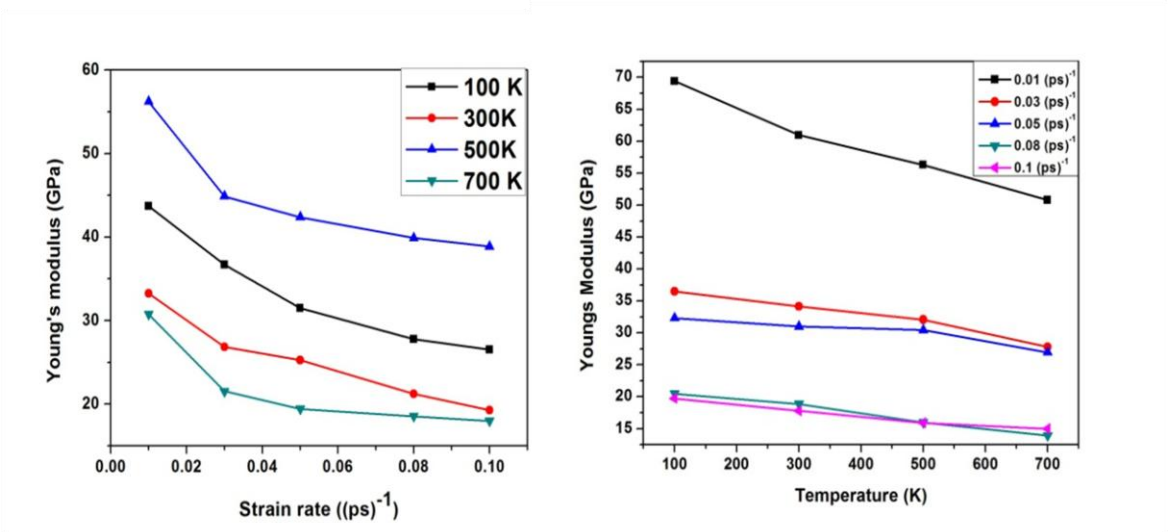

Fig. 4.9 Variation of Young's modulus of Pd nanowire: (a) Strain rates (b) Temperature.

Table 4.8 Young's modulus variation w.r.t Strain rate for Pd nanowire

Strain Rate (ps^{-1})	**E (100K) (GPa)**	**E (300K) (GPa)**	**E (500K) (GPa)**	**E (700K) (GPa)**
0.01	69.38	60.94	56.29	50.80
0.03	36.46	34.14	32.07	27.78
0.05	32.29	31.60	30.44	26.96
0.08	20.45	18.84	15.98	13.92
0.1	19.74	17.78	15.92	14.97

Table 4.9 Young's modulus variation w.r.t temperature for Pd nanowire

Temperature (K)	**E ($0.01ps^{-1}$) (GPa)**	**E ($0.03ps^{-1}$) (GPa)**	**E ($0.05\ ps^{-1}$) (GPa)**	**E ($0.08\ ps^{-1}$) (GPa)**	**E ($0.1\ ps^{-1}$) (GPa)**
100K	43.71	36.67	31.49	27.77	26.51
300K	33.25	26.84	25.27	21.23	19.27
500K	56.21	44.88	42.38	39.88	38.88
700K	30.76	21.54	19.43	18.54	17.98

4.2.5 Strain rate sensitivity (m) variation plot

From Fig 4.10, we detect the variations of strain rate sensitivity values w.r.t temperature and log-log plot for flow stress and strain rate. In Fig 4.10 (a), the progressive trend is observed which is quite specific. The variation of 'm' w.r.t temperature is quite fluctuating unlike we

observed in Pt nanowire. The variations are due to presence of twinned faceted structure which can be recognized as stress concentration at the junction between coherent twin boundaries and surface facet [34]. The detailed values are depicted in Table 4.10.

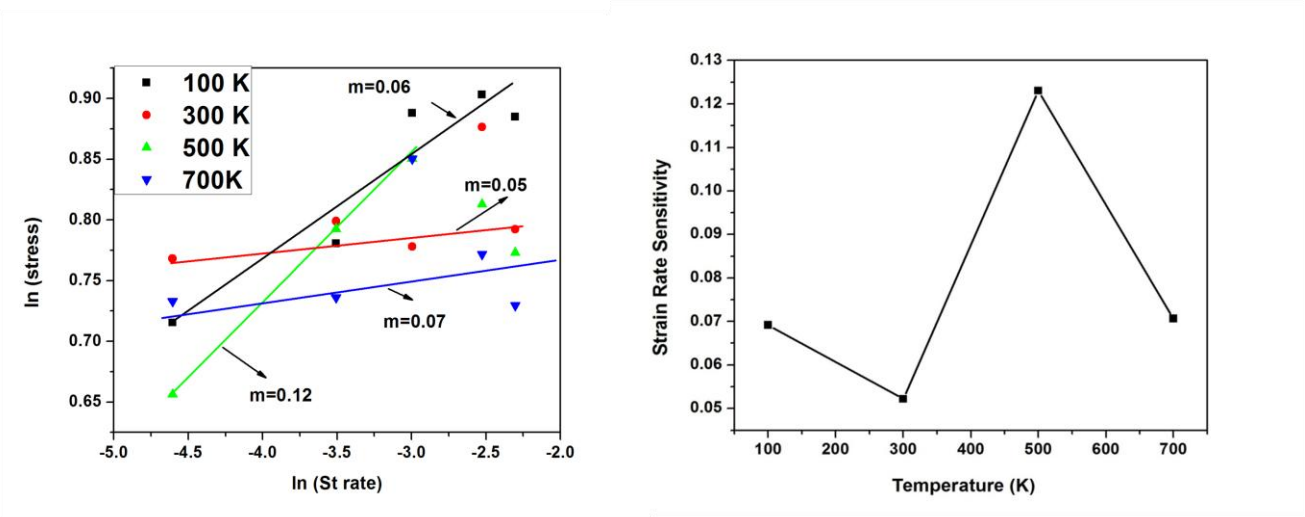

Fig4.10 Plots for Pd nanowire: (a) ln(stress) vs ln(strain rate) (b) m vs Temperature.

Table 4.10 Strain rate sensitivity variation w.r.t temperature for Pd nanowire

Temperature (K)	Strain Rate Sensitivity
100	0.06
300	0.05
500	0.12
700	0.07

4.3 Pd_{50}-Pt_{50} alloy nanowire

4.3.1 Stress-Strain plot

In the Figure 4.11 the stress-strain relationship of the Pd_{50}-Pt_{50}-nanowire, simulated at 100 K, 300 K, 500 K, and 700 K each for strain rates of 1%, 3%, 5%, 8% and 10% ps^{-1}, respectively is depicted. The nature of stress-strain curve is as similar as that obtained in the previous segments i.e. in Pt and Pt nanowires. However, the mechanical properties like yield strength and elastic modulus varies. The basic trend observed is, with the progressive strain rate the yield strength increases at a particular temperature condition. With the increase in temperature condition the yield strength decreases w.r.t it's lower temperature conditions [26]. Further details are evaluated in the following sections.

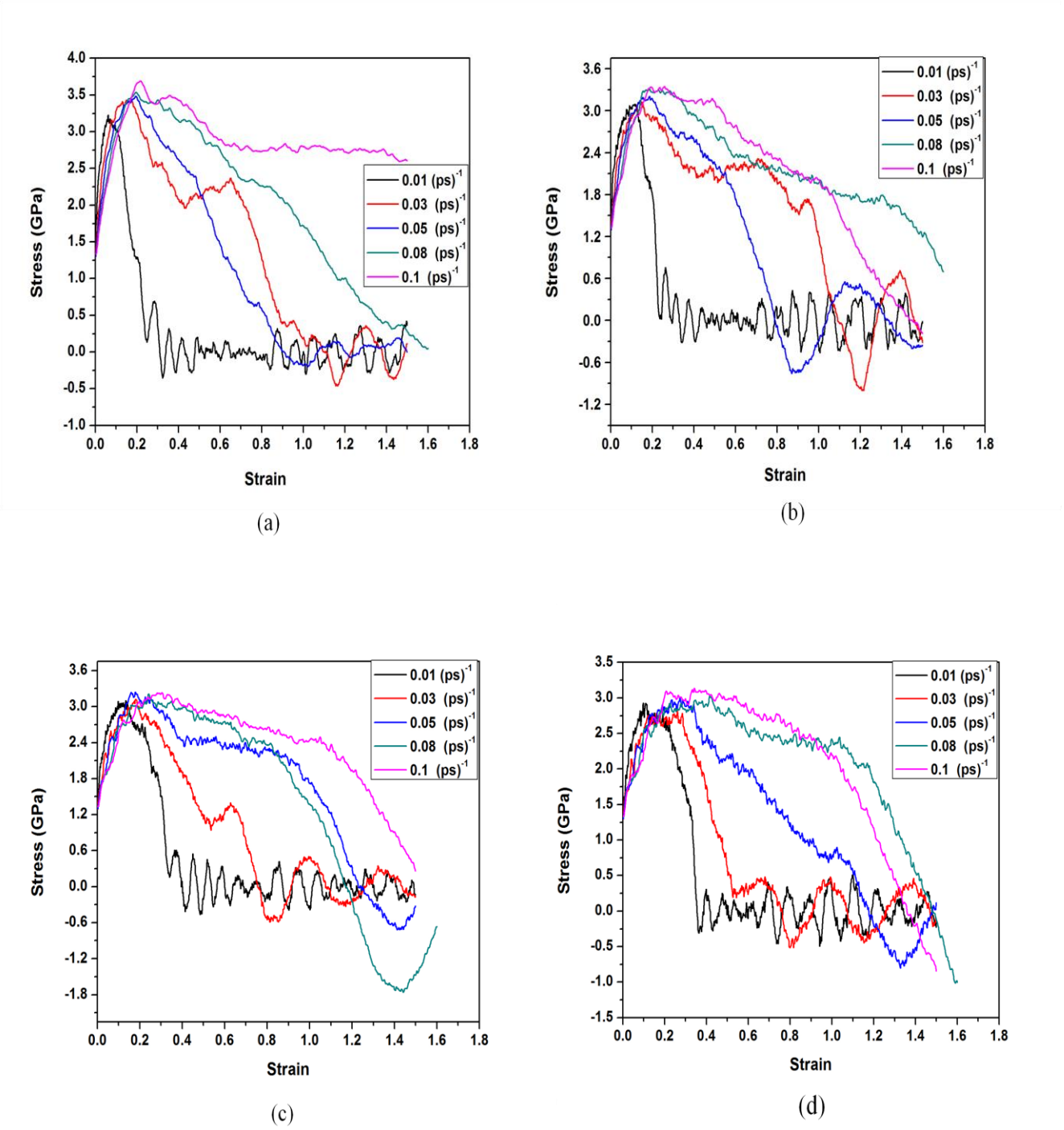

Fig. 4.11 Stress-Strain plot of Pd_{50}-Pt_{50} nanowire deformed at (a) 100 K (b) 300 K (c) 500 K (d) 700 K temperatures. Each sampleis deformed at the strain rate ranging from 1% to 10% ps^{-1}.

4.3.2 VMD snapshots

The visual molecular dynamics (VMD) software is used in viewing the activities of molecular dynamics simulations. The equivalent atomic activities were shown in Fig.4.2, in different strain conditions. We observe that at strain value 0, the Pd_{50}-Pt_{50} nanowire is in perfect crystalline form. Subsequently, with the increase in strain values the nanowire deforms and at the strain value 0.294 the necking phenomenon is observed which corresponds to ductility. Fracture occurs at the strain value of 0.4.From the previous sections we observe that, after alloying the nanowire; it yields early as compared to that of Pd, Pt nanowires.

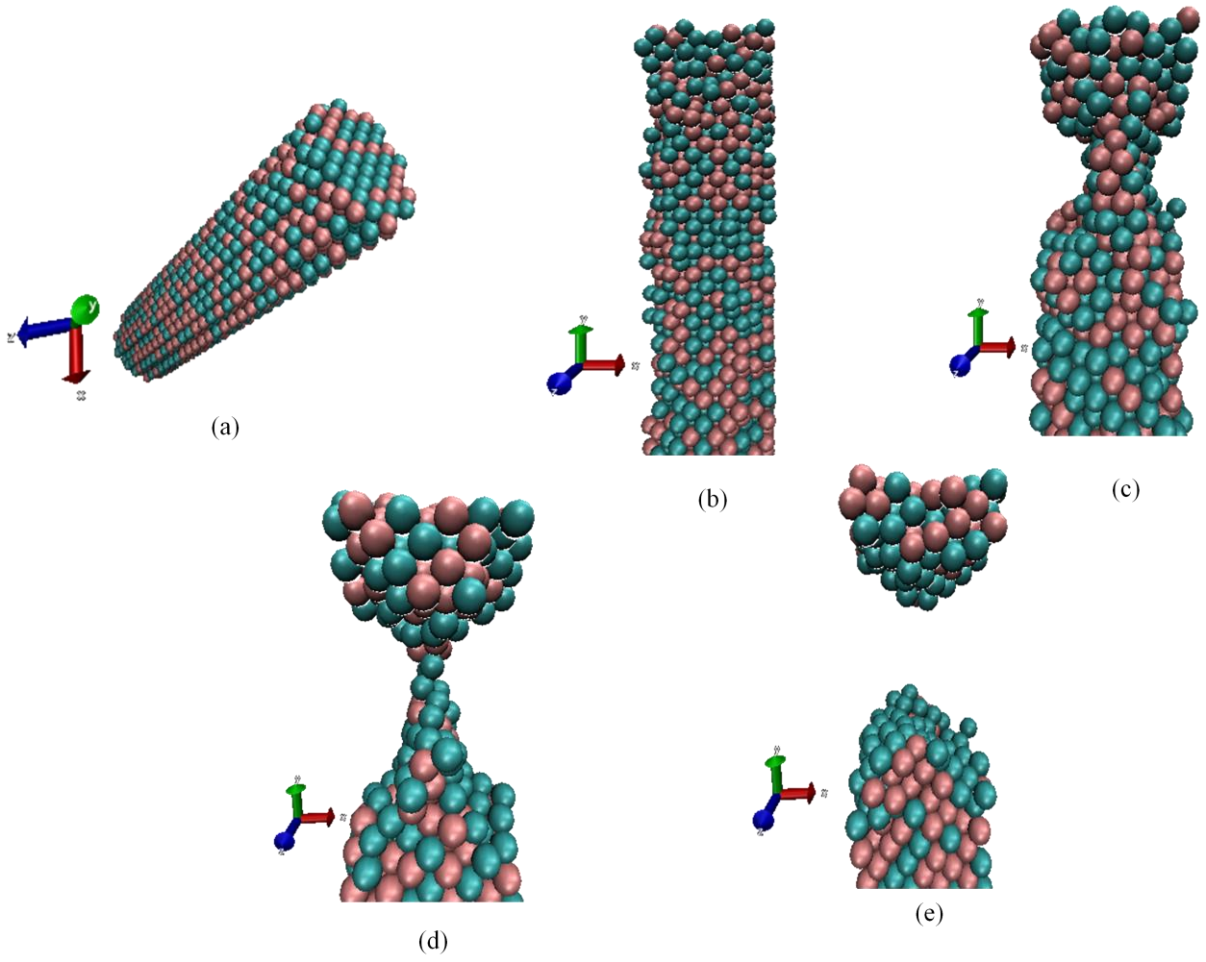

Fig.4.12. VMD snapshots of deformed Pd_{50}-Pt_{50} nanowire at different strain condition (strain rate= 0.01 ps^{-1} and 100 K temperature) (a) 0 (b) 0.06 (c) 0.2 (d) 0.294 (e) 0.4.

4.3.3 Yield Strength variation

MD simulation results focused on the effect of yield strength due to the variation in strain rate and temperature is discussed in the following sections.

4.3.3.1 Effect of strain rate

In the fig 4.13 (a), the depiction of yield strength w.r.t temperature and strain rate is observed as follows. The nanowire deformed at lower strain rate and lower temperature condition exhibits higher yield strength compared to that of higher temperature conditions sample. With the increase in strain rate, yield strength too increases. The trend seen in the figure is progressive in nature; the reason justifying this behaviour is, at lower temperature the barrier for dislocations is prevailing. However, with increase in temperature; the mobility of dislocations is easier which corresponds to supportive deformation and lower yield strength. The detailed values are depicted in Table 4.11.

4.3.3.2 Effect of Temperature

The decreasing trend is observed in fig 4.13 (b) with the increase in temperature condition irrespective of the strain rate deformation. It must be noted that lower strain rate has lower yield strength value. However, increasing the strain rate deformation increases the yield strength. The reason for the same is already discussed in the previous sections. The detailed values are depicted in Table 4.12.

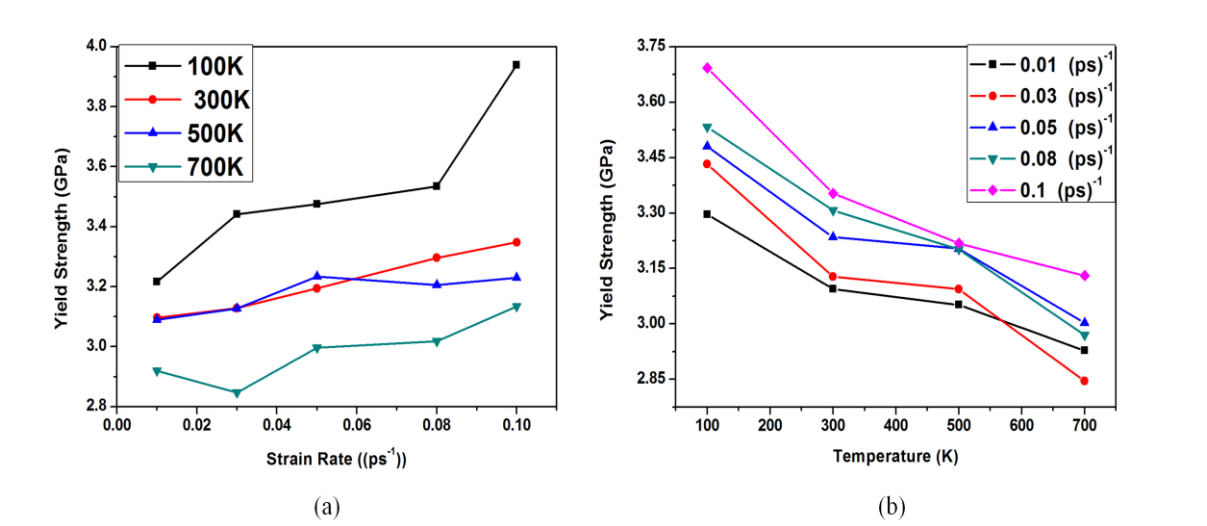

Fig.4.13.Variation of yield strength of Pd-Pt nanowire: (a) Strain rates (b) Temperature.

Table 4.11 Yield strength variation w.r.t Strain rate for Pd-Pt alloy nanowire

Strain Rate (ps^{-1})	**Yield Strength (100K) (GPa)**	**Yield Strength (300K) (GPa)**	**Yield Strength (500K) (GPa)**	**Yield Strength (700K) (GPa)**
0.01	3.21	3.09	3.08	2.91
0.03	3.44	3.12	3.12	2.84
0.05	3.47	3.19	3.23	2.99
0.08	3.53	3.29	3.20	3.01
0.1	3.69	3.34	3.22	3.13

Table 4.12 Yield strength variation w.r.t Temperature for Pd-Pt alloy nanowire

Temperature (K)	**Yield Strength ($0.01\ ps^{-1}$) (GPa)**	**Yield Strength ($0.03ps^{-1}$) (GPa)**	**Yield Strength ($0.05ps^{-1}$) (GPa)**	**Yield Strength ($0.08ps^{-1}$) (GPa)**	**Yield Strength ($0.1ps^{-1}$) (GPa)**
100K	3.29	3.43	3.48	3.53	3.69
300K	3.09	3.12	3.23	3.30	3.35
500K	3.05	3.09	3.20	3.20	3.21
700K	2.92	2.84	2.96	2.96	3.13

4.3.4 Elastic Modulus variation

MD simulation results focused on the effect of Young's modulus due to the variation in strain rate and temperature is discussed in the following sections.

4.3.4.1Effect of Strain Rate

The effect of strain rate on Young's modulus (E) is presented by plotting the graph of E vs strain rate as shown in Fig.4.9 (a). The straight line with a constant slope for any given temperature with decreasing trend is roughly presented in Fig. 4.9. At lower strain rate and lower temperature the value of elastic modulus is high. Subsequently, it decreases with increase in temperature condition. Conventionally, the trend is quite justified; lower temperature makes a nanowire quite stiff which corresponds to higher elastic modulus. The detailed values are depicted in Table 4.13.

4.3.4.2 Effect of Temperature

In Fig 4.9 (b), we clearly observe the declining trend with the increase in temperature. At lower strain rate and low temperature condition the value of elastic modulus is quite high and reduces with the increase in strain rate at the same temperature condition. The trend observed in the figure is justified conventionally using softening and stiffness phenomenon as described in the previous sections except the 3% ps^{-1} strain rate condition, which still under investigation. The detailed values are depicted in Table 4.14.

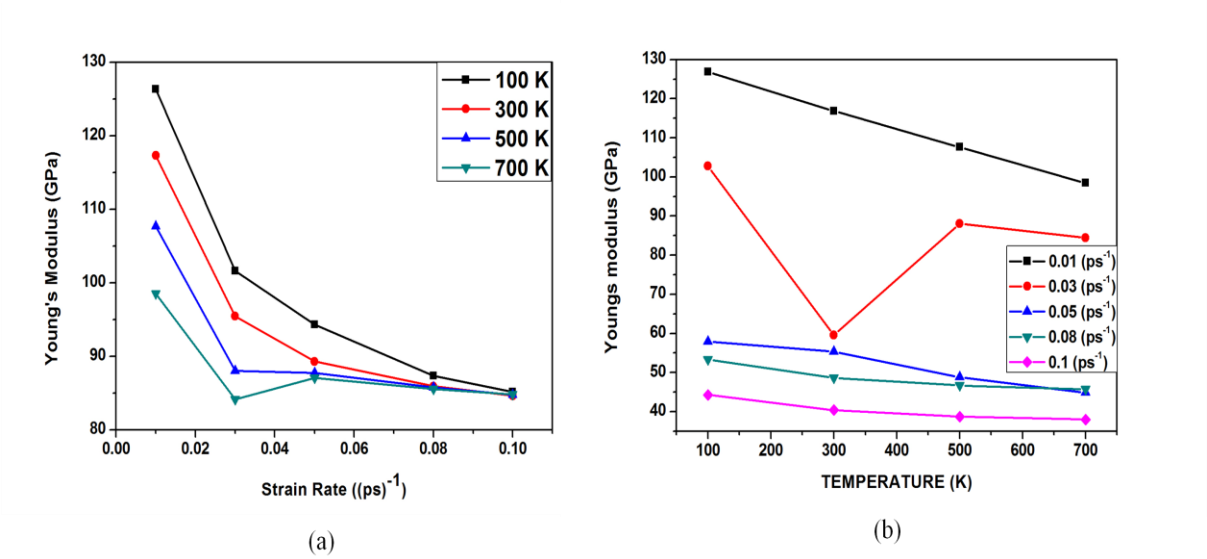

Fig. 4.14 Variation of Young's modulus of Pd-Pt nanowire: (a) Strain rate (b) Temperature.

Table 4.13 Young's modulus variation w.r.t Strain rate for Pd-Pt alloy nanowire

Strain Rate (ps^{-1})	**E (100K) (GPa)**	**E (300K) (GPa)**	**E (500K) (GPa)**	**E (700K) (GPa)**
0.01	126.87	116.87	107.63	98.44
0.03	102.82	59.59	88.67	84.40
0.05	57.90	55.33	48.81	44.87
0.08	53.33	48.68	46.68	45.70
0.1	44.27	40.40	38.72	37.97

Table 4.14 Young's modulus variation w.r.t temperature for Pd-Pt alloy nanowire

Temperature (K)	E ($0.01\ ps^{-1}$) (GPa)	E ($0.03\ ps^{-1}$) (GPa)	E ($0.05\ ps^{-1}$) (GPa)	E ($0.08\ ps^{-1}$) (GPa)	E ($0.1ps^{-1}$) (GPa)
100K	126.36	101.64	94.31	87.32	85.14
300K	117.29	95.45	89.29	85.91	84.62
500K	107.65	88.63	87.75	85.75	84.75
700K	98.54	84.16	87.04	85.55	84.81

4.3.5 Strain rate sensitivity variation plot

The trend observed in Fig 4.15 (a) is justified according to the literature [34]. This figure illustrates the log-log plot between flow stress and strain rate. In Fig 4.15 (b), the variation of 'm' is quite similar when compared to that of Pt and Pd nanowires. The cause for this phenomenon is explained and illustrated in the above sections [33]. The detailed values are depicted in Table 4.15.

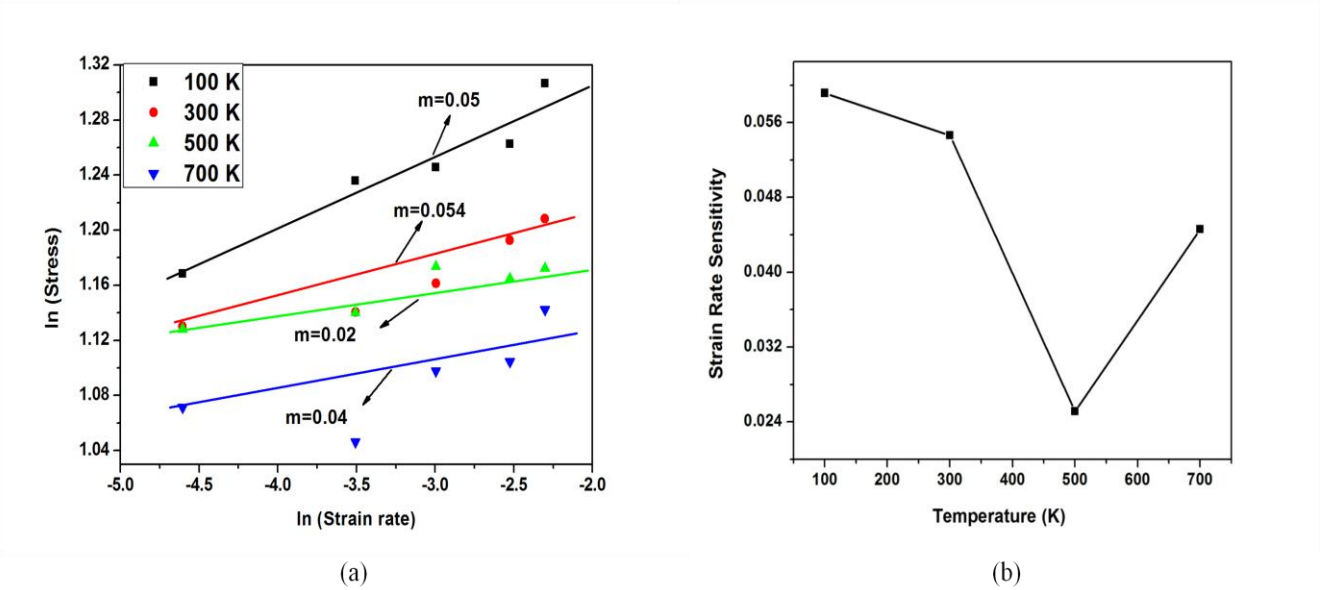

(a) (b)

Fig 4.15 Plots for Pd-Pt alloy nanowire (a) ln(stress) vs ln(strain rate) (b) m vs Temperature.

Table 4.15 Strain rate sensitivity variation w.r.t temperature for Pd-Pt alloy nanowire

Temperature (K)	**Strain Rate Sensitivity**
100	0.05
300	0.054
500	0.02
700	0.04

Chapter-5

Conclusions

Conclusions

a) With the increase in temperature, yield strength and elastic modulus values decreases for Pd, Pt, and Pd-Pt alloy nanowires.
b) With the increase in strain rates, yield strength values increases but elastic modulus decreases in Pd, Pt, and Pd-Pt alloy nanowires.
c) Log-log plot of stress vs strain rate always exhibits the positive slopes for Pd, Pt, and Pd-Pt alloy nanowires.
d) Strain rate sensitivity variations with respect to temperature exhibits different trend for the all Pt, Pt, and Pd-Pt alloy nanowires. ‘m’ value for the Pd-Pt alloy nanowire shows completely different behaviour as compared to Pd and Pt single crystal nanowire.

Chapter-6

References

References

[1] A.R Setoodeh, H Attariani, M.Khosrownjad; Computational Material science, 44 (2008) 378-384.

[2] Christopher R.Weinberger and Wei Cai; J.mater chem., 2012, 22, 3277.

[3] Chi Yan Tang, L.C.Z Hang, Kausala Mylvaganam; Computational Material Science, 51 (2012) 117-121.

[4] J. Bürki, C. A. Stafford, D. L. Stein, Phys Rev Lett, 95 (2005), 090601 Doi:10.1002/adma.200390087.

[5] A. Bietsch, B. Michel, Appl Phys Lett, 80 (2002), 3346.

[6] Subramanian K. R. S. Sankaranarayanan, Venkat R. Bhethanabotla, and Babu Joseph; Phy Rev Lett, 76(2007), 134117.

[7] S.J.A. Koh, H.P.Lee, C.Lu, and Q.H.Cheng; Phy Rev Let, 72 (2005) 085414.

[8] Hillie, T., & Hlophe, M. (2007). Nanotechnology and the challenge of clean water, *Nature nanotechnology, 2*(11), 663-664.

[9] Amir Dindar, Shoeb Roman; University of South Alabama, 2005.

[10] Lu, Y., Peng, C., Ganesan, Y., Huang, J. Y., & Lou, J. (2011); *Nanotechnology, 22*, 355702.

[11] Zhu, Xu, Qin, Fung, & Lu (2009), *Nano Letters, 9*(11), 3934-3939.

[12] Richter G., Hillerich, K., Gianola, D. S., Mo nig, R., Kraft, O., &Volkert, C. A. (2009); *Nano Letters, 9*(8), 3048-3052.

[13] Seo, J. H., Yoo, Y., Park, N. Y., Yoon, S. W., Lee, H., Han, S.,Ahn, J. P. (2011); *Nano Letters, 11*(8), 3499-3502.

[14] Wu, Z., Zhang, Y. W., Jhon, M. H., Gao, H., & Srolovitz, D. (2012); *Nano Letters, 12*(2), 910-914.

[15] Wu, H. (2006). Molecular; *Mechanics Research Communications, 33*(1), 9-16.

[16] Diao, J., Gall, K., Dunn, M., & Zimmerman, J. (2006); *ActaMaterialia, 54*(3), 643-653.

[17] Park, H., & Klein, P. (2007); *Physical Review B, 75*(8), 85408.

[18] A.R. Setoodeh, H. Attariani, M. Khosrownejad; Computational Materials Science 44 (2008) 378–384.

[19] Yajun Gao, Hongbo Wang, Jianwei Zhao, Changqing Sun, Fengyin Wang; Computational Materials Science 50 (2011) 3032–3037.

[20] Komanduri, R., Chandrasekaran, N., & Raff, L. (2001); *International Journal of Mechanical Sciences, 43*(10), 2237-2260.

[21] Weinberger, C. R., & Cai, W. (2012); *Journal of Materials Chemistry*.

[22] Koh, A., & Lee, H. (2006); *Nano Letters, 6*(10), 2260-2267.

[23] A. Alavizargara, K. Mirabbaszadehb, A. Baktasha, A. Sasanic; Proceedings of the 4th International Conference on Nanostructures (ICNS4)12-14 March, 2012, Kish Island, I.R. Iran.

[24] Kawamura, M., Paul, N., Cherepanov, V., &Voigtländer, B. (2003); *Physical Review Letters, 91*(9), 96102.

[25] Yang, Y., Callegari, C., Feng, X., Ekinci, K., & Roukes, M. (2006); *Nano Letters, 6*(4), 583-586.

[26] Jijun Lao, Mehdi Naghdi Tam, Dinesh Pinisetty, and Nikhil Gupta; Department of Mechanical and Aerospace Engineering, Polytechnic Institute of New York University, Brooklyn, NewYork, U.S.A, A Review.

[27] S. J. A. Koh, H. P. Lee, C. Lu, Q. H. Cheng, Phys Rev B, 72 (2005), 085414.

[28] M. S. Daw, M. I. Baskes, Phys Rev Lett, 50 (1983), 1285.

[29] H.F. Zhan, Y.T. Gu; The International Conference on Computational Methods, NOVEMBER 15-17, 2010, Zhangjiajie, China.

[30] R. A. Vasin, F. U. Enikeev, M. I .Mazurski; JOURNAL OF MATERIALS SCIENCE 33 (1998) 1099-1103.

[31] E. Karimi, A. Zarei-Hanzaki, M.H. Pishbin, H.R. Abedi, P. Changizian; Materials and Design 49 (2013) 173–180.

[32] Haifei Zhan, Doctor of Philosophy thesis, School of Physics, Chemistry and Mechanical Engineering Science and Engineering Faculty Queensland University of Technology, http://eprints.qut.edu.au.

[33] Gemma Safont Camprubí Lund University; 2011.

[34] Chuang Deng and Frederic Sansoz, Phys Rev lett, 81 (2010), 155430.

[35] Dan Huang, Qing Zhang, Pizhong Qiao, Computational Materials Science, 50 (2011) 903–910.